IEEE Access
Multidisciplinary | Rapid Review | Open Access Journal

SPECIAL SECTION ON CYBER-PHYSICAL SYSTEMS

Received August 22, 2018, accepted September 16, 2018, date of publication October 1, 2018, date of current version October 25, 2018.

Digital Object Identifier 10.1109/ACCESS.2018.2872935

Performance Analysis of DF/AF Cooperative MISO Wireless Sensor Networks With NOMA and SWIPT Over Nakagami-*m* Fading

DUC-DUNG TRAN[1], DAC-BINH HA[1], VAN NHAN VO[2,3], CHAKCHAI SO-IN[3], (Senior Member, IEEE), HUNG TRAN[4], TRI GIA NGUYEN[5], ZUBAIR AHMED BAIG[6], AND SURASAK SANGUANPONG[7]

[1]Faculty of Electrical & Electronics Engineering, Duy Tan University, Danang 550000, Vietnam
[2]International School, Duy Tan University, Danang 550000, Vietnam
[3]Applied Network Technology Laboratory, Department of Computer Science, Faculty of Science, Khon Kaen University, Khon Kaen 40002, Thailand
[4]School of Innovation, Design and Engineering, Mälardalen University, 72123 Västerås, Sweden
[5]Faculty of Information Technology, The University of Danang - University of Science and Education, Danang 550000, Vietnam
[6]CSIRO, Data61, Melbourne, VIC 3008, Australia
[7]Department of Engineering, Faculty of Engineering, Kasetsart University, Bangkok 10900, Thailand

Corresponding author: Chakchai So-In (chakso@kku.ac.th)

This work was supported in part by Enthuse Company Ltd. under Grant Ent-KKU-2560-01, in part by Khon Kaen University, and in part by Kasetsart University. The work of D.-B. Ha was supported by the Vietnam National Foundation for Science and Technology Development under Grant 102.04-2017.301. The work of H. Tran was supported by the SSF Framework Grant Serendipity.

ABSTRACT In this paper, we investigate downlink cooperative multiple-input single-output wireless sensor networks with the nonorthogonal multiple access technique and simultaneous wireless information and power transfer over Nakagami-*m* fading. Specifically, the considered network includes a multiantenna sink node, an energy-limited relay cluster, a high-priority sensor node (SN) cluster, and a low-priority SN cluster. Prior to transmission, a transmit antenna, a relay, a high-priority SN, and a low-priority SN are selected. In this paper, we propose three antenna-relay-destination selection schemes, i.e., sink node-high-priority, sink node-relay, and sink node-low-priority. In each proposed scheme, we consider two relaying strategies, i.e., decode-and-forward and amplify-and-forward, and then, we derive the corresponding closed-form expressions of outage probability at the selected SNs. In addition, we introduce two algorithms: 1) the power-splitting ratio optimization algorithm and 2) the best antenna-relay-destination selection determination algorithm. Finally, we utilize the Monte Carlo simulations to verify our analytical results.

INDEX TERMS Cooperative transmission, energy harvesting, nonorthogonal multiple access, successive interference cancellation, wireless sensor networks.

I. INTRODUCTION

In recent years, Industry 4.0 has been attracting considerable attention from researchers in both industry and academia due to its reduced energy consumption and increased economic benefits [1], [2]. Furthermore, Internet of Things (IoT) has emerged as a basic premise enabling the implementation of Industry 4.0 [3], [4]. In the progress of the IoT paradigm, wireless sensor networks (WSNs) have played a vital role in connecting billions of devices over the Internet for applications including healthcare services, transportation, process analysis, and environmental assessment [5].

A WSN is composed of sensor nodes (SNs) that have the ability to sense their environment, perform computations and communicate [6]. However, the lifetime of WSNs is limited due to the energy restriction at sensor nodes (SNs) [7], [8]. To overcome this limitation, there have been many studies on reducing the energy consumption in WSNs [9], [10]. For example, in [9], the issue of prolonging the lifetime of cluster-based WSNs with the LEACH protocol was investigated. In [10], a protocol of transmission power control through a reinforcement learning process was proposed. Although the above studies can improve the lifetime of WSNs, recharg-

ing or replacing batteries in SNs is still necessary. Moreover, this task incurs a high cost, and it can be hazardous for humans to replace batteries manually (e.g., in nuclear reactors or toxic environments) or difficult to implement (e.g., inside the human body) [11].

Therefore, the question of how to prolong the lifetime of SNs with more effective recharging methods or without replacing batteries arises. The wireless power transfer (WPT) technique has recently been considered to be a promising solution [12]–[14]. It is especially attractive for IoT devices or WSNs [15]. In this approach, SNs can harvest energy from ambient radio frequency (RF) energy sources (e.g., Wi-Fi, digital television (DTV) bands or surrounding mobile electronic devices) and use the collected energy to power their operations [16]. Furthermore, WPT has been demonstrated as a solution for overcoming the limitations of conventional energy harvesting (EH) methods (e.g., solar, wind, or external charging methods), which are only applicable in certain environments due to their intermittent and unpredictable nature [17]. However, a crucial challenge for WPT is the rapid reduction in energy transfer efficiency over the transmission distance due to the propagation loss, leading to the limited application of WPT [17], [18]. Consequently, simultaneous wireless information and power transfer (SWIPT) has recently been proposed to improve the energy transfer efficiency [17], [18]. In SWIPT, both energy and information can be transmitted simultaneously by the same RF signal.

Cooperative relaying transmission is also an alternate approach for increasing the lifetime of SNs by using intermediate relay nodes to reduce the transmission distance and total energy consumption [19], [20]. Furthermore, this approach can help improve the transmission reliability and increase the coverage area of wireless networks. Unfortunately, relays are often the energy-constrained nodes. Therefore, energy is also a vital challenge in cooperative communication.

To overcome this limitation, the application of SWIPT to cooperative networks has recently been explored [21]–[23]. For example, Xiong *et al.* [22] investigated the application of SWIPT in a nonregenerative multiple-input multiple-output orthogonal frequency-division multiplexing (MIMO-OFDM) relaying system. Two practical receiver architectures based on two relaying protocols, namely, time-switching-based relaying (TSR) and power-splitting-based relaying (PSR), were considered. Do *et al.* [23] investigated the system performance of opportunistic scheduling in dual-hop cooperative networks with SWIPT over a Rayleigh fading channel. In this context, the PSR protocol and relaying strategies, i.e., decode-and-forward (DF), variable-gain amplify-and-forward (VG-AF), and fixed-gain amplify-and-forward (FG-AG), were examined.

In addition to the energy constraint, WSNs face computing capability and bandwidth limitations [24]–[26]. In particular, the applications of WSNs in IoT, military and surveillance systems require ultra-low latency and ultra-high connectivity [27], [28]. Nonorthogonal multiple access (NOMA) has recently been proposed as a promising multiple access technique for future wireless networks [29]–[31]. This is because NOMA provides better spectrum efficiency and supports a massive connection compared with the conventional OMA technique [32]–[36].

For example, Shimojo *et al.* [35] showed that NOMA outperforms OMA in terms of sum rate. Saito *et al.* [34] investigated a NOMA system that consists of a single transmitter and two user equipments (UEs). They reported that the user rate gains of NOMA from orthogonal frequency-division multiple access (OFDMA) are 32% and 48% for the two users. Shimojo *et al.* [35] concluded that NOMA can achieve better performance gains than OMA and can improve the user throughput by 34.2% under a specific setting. Therefore, NOMA is considered to be a sustainable solution for overcoming the above limitation in WSNs [37], [38].

Recently, there have been many works studying cooperative networks with NOMA and SWIPT [30], [39], [40]. Specifically, in [30], a cooperative SWIPT NOMA protocol, in which nearby NOMA users that are close to the source act as EH relays to help those further away, was proposed. The work in [39] investigated the outage performance of a SWIPT-based cooperative NOMA system consisting of one source, multiple energy-constrained relays, and two destinations. However, both works [30], [39] only consider the single-input single-output (SISO) system, DF relaying strategy, and Rayleigh fading channel.

In [40], a SWIPT-based cooperative multiple-input single-output (MISO) NOMA system with two users, cell-center and cell-edge users, was considered. The authors focused on improving the performance of the cell-edge user by using transmit antenna selection (TAS) at the source and SWIPT-based cooperative transmission. In this context, the cell-center is considered to be an energy-constrained DF relay that helps the source forward information to the cell-edge user. Nevertheless, this work only investigates a simple system model consisting of one source and two users, in which only the performance of one user, i.e., the cell-edge user, is evaluated. In addition, it only considers the DF protocol for relaying transmissions and the Rayleigh fading scenario.

To the best of our knowledge, investigations on combining NOMA and SWIPT for cooperative MISO WSNs over a Nakagami-*m* fading channel have not been conducted. Therefore, this research focuses on analyzing the performance of DL cooperative MISO WSNs with NOMA and SWIPT. In the considered network, a multiantenna sink node communicates with two SN clusters directly and with the help of energy-constrained relays using NOMA over a Nakagami-*m* fading channel. It is noted that Nakagami-*m* is considered a general channel model that can include the well-known Rayleigh and Rician fading channels. Prior to transmission, the transmit antenna, SN, and relay selection strategies are performed. In this setting, TAS is used since it is considered a low-complexity and power-efficient communication solution for the sink node (source) with multiple antennas [41], [42].

Furthermore, this scheme can improve the system performance and guarantee a good trade-off between the diversity gain and the implementation cost [43]. The main contributions of our paper are summarized as follows:

- We propose a new model of DL cooperative MISO WSN with NOMA and SWIPT over a Nakagami-*m* fading channel.
- We propose three antenna-relay-destination selection strategies, i.e., sink node−high-priority SN (SHS), sink node−relay (SRS), and sink node−low-priority SN (SLS), and conduct performance comparisons.
- We derive the closed-form expressions of outage probability (OP) for the three strategies in the case of using DF and amplify-and-forward (AF) relaying strategies.
- We propose two algorithms: (i) power-splitting ratio optimization for minimizing OP and (ii) average transmit signal-to-noise ratio (SNR) threshold determination for determining which of the three proposed solutions provides the best performance for SNs.

The remainder of this paper is organized as follows. Section II briefly reviews some of the related works on cooperative SWIPT and NOMA in WSNs. In Section III, the system model, our proposed solutions, and the cooperative communication process are provided in detail. Sections IV and V analyze the performance of the considered system using DF and AF relaying protocols. In Section VI, optimization of the power-splitting ratio and the strategy for effective communication are investigated. In Section VII, the numerical results and discussion are presented. Finally, conclusions and future extensions are summarized in Section VIII.

II. RELATED WORK

In this section, we briefly present some related works on SWIPT and NOMA that include a cooperative approach in WSNs. There have been several works regarding SWIPT in WSNs to prolong the lifetime of SNs in recent years [44]–[47]. Specifically, Kisseleff *et al.* [44] proposed a new wireless EH method for magnetic induction (MI)-wireless underground sensor networks (WUSNs) based on simultaneous signal transmissions from multiple SNs with optimized signal constellations. Meanwhile, Pan *et al.* [45] analyzed the performance of SWIPT in WSNs, where a mobile reader broadcasts a command with RF energy to SNs. SNs then deliver their information to the reader over orthogonal channels by using the harvested energy. However, the above studies only consider direct communication.

Cooperative SWIPT was investigated in [46] and [47]. Guo *et al.* [46] studied the application of SWIPT to cooperative clustered WSNs, where relay nodes harvest the ambient RF signal and use the harvested energy for their relaying transmission. Liu *et al.* [47] also proposed a novel cooperative SWIPT scheme for wirelessly powered sensor networks (WPSNs). In this context, a conflict-free schedule initialization algorithm, a resource allocation problem to maximize the network energy efficiency, and a heuristic algorithm were presented. Nevertheless, these works do not consider the multiple-antenna scheme or optimization of the power-splitting ratio.

Regarding NOMA in WSNs, Anwar *et al.* [37] investigated the performance of NOMA for DL ubiquitous WSNs (UWSNs), where SNs experience interference from other devices sharing the same spectrum. In this work, comparisons of the obtained throughput and energy consumption efficiency between NOMA and conventional OMA were presented. However, the authors did not consider the RF EH issue for SNs. Song and Zheng [38] also studied a WPSN, where SNs collect energy from an access point (AP) and then use the collected energy to transmit information to the AP by applying the NOMA technique. However, this study did not investigate SWIPT and relaying transmission.

Motivated by the aforementioned works, in this paper, we investigate the application of NOMA and SWIPT in DL cooperative WSNs.

TABLE 1. Notations.

Notations	Meaning
h_{AB}	The channel coefficient of the link from transmitter A to receiver B.
m_{AB}	Nakagami-m fading parameter of the link from transmitter A to receiver B.
$\mathbb{E}[\cdot]$	The expectation operator.
$\lvert\cdot\rvert$	The absolute value.
$\mathcal{CN}(0, N_0)$	A scalar complex Gaussian distribution with zero mean and variance N_0.
ρ	Power-splitting ratio.
η	Energy conversion efficiency.
P_S	Transmit power at sink node.
S_c	Sink node with the selected transmit antenna.
H_c and L_c	The selected SNs.
R_c	The selected relay.
a_{H_c} and a_{L_c}	Power allocation coefficients for SNs H_c and L_c at sink node S_c.
b_{H_c} and b_{L_c}	Power allocation coefficients for SNs H_c and L_c at relay R_c.
γ_S	Average transmit signal-to-noise ratio (SNR).
$\mathcal{E}$	The harvested energy.
$\mathcal{K}(\cdot)$	The ν^{th}-order modified Bessel function of the second kind.
$\mathcal{O}$	Outage probability.
$\nabla\mathcal{O}$	The gradient of $\mathcal{O}$.
$\dot{y}$	The first-order derivative of function y.

III. SYSTEM MODEL

For clarity, we define in Table 1 the notations adopted in the following part of this paper.

As depicted in Fig. 1, we study a DL NOMA cooperative WSN that consists of one sink node, denoted by S; one cluster of K SNs considered as energy-constrained relays, denoted by $R = \{R_1, \ldots, R_K\}$; one cluster of P high-priority SNs, denoted by $H = \{H_1, \ldots, H_P\}$; and one cluster of Q low-priority SNs, denoted by $L = \{L_1, \ldots, L_Q\}$. Sink node S is equipped with N antennas, whereas the remaining devices are equipped with a single antenna due to the size limitation of SNs. In the investigated network, we focus on DL transmission, in which sink node S intends to transmit control information to SNs in clusters H and L by using

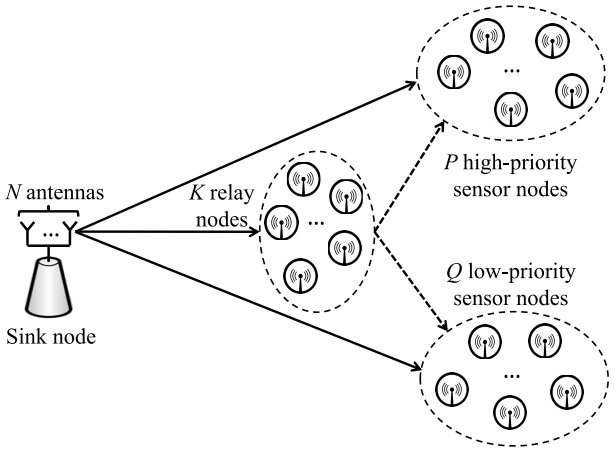

FIGURE 1. The system model of DL MISO cooperative WSN with NOMA and SWIPT.

NOMA. Specifically, SNs in cluster H are assigned to collect the important data, e.g., sensing smoke to alert of a forest fire. Meanwhile, SNs in cluster L are used for collecting basic information, such as temperature or humidity. To improve the received signal quality at the SNs, relaying transmission is used. However, the relays (i.e., K SNs in cluster R) have limited energy. In this context, the SWIPT technique, in which the sink node S not only transmits information to the SNs and relays but also broadcasts energy to the relays, is considered.

Suppose that h_{AB} ($A \neq B, A \in \{S_n, R_k\}, B \in \{R_k, H_p, L_q\}$, $1 \leq n \leq N$, $1 \leq k \leq K$, $1 \leq p \leq P$, $1 \leq q \leq Q$) denotes the channel coefficient of the $A \rightarrow B$ link. Herein, h_{AB} is an independent identically distributed (i.i.d.) random variable (RV) following a Nakagami-m distribution with parameter m_{AB} and mean value $\Omega_{AB} = \mathbb{E}\left[|h_{AB}|^2\right]$, where $\mathbb{E}[\cdot]$ denotes the expectation operator. Thus, the channel power gain $|h_{AB}|^2$ is an i.i.d Gamma RV [48].

The system operation is briefly depicted as follows:

- Antenna-relay-destination selection: the selection will be performed prior to transmission. Specifically, we propose some solutions to choose a transmit antenna, a relay, and SNs in clusters H and L based on the respective channel gains. Further analysis will be presented in the next subsection.
- Cooperative communication process: after antenna-relay-destination selection, this process is performed in two phases. In the first phase, the sink node intends to communicate with two selected destinations (i.e., SNs in clusters H and L) using NOMA. At the selected relay, it uses the PSR protocol, as shown in Fig. 2, for EH and information processing. In the second phase, the relay uses all the harvested energy from the first phase to forward the received signals to the chosen destinations by applying either the DF or AF relaying protocol. At the destination, the received signals (i.e., direct signal and relaying signal) are processed by employing the selection combining (SC) scheme.

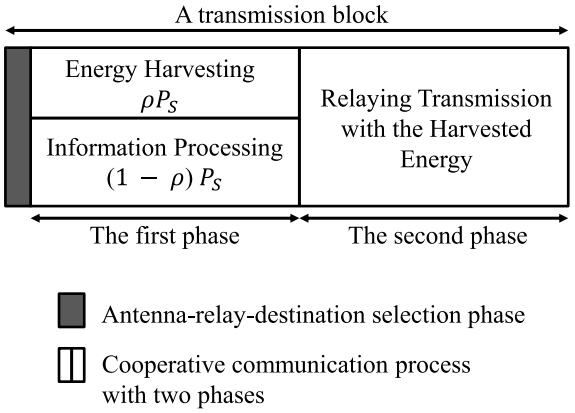

FIGURE 2. Illustration of system operation with the PSR protocol.

A. ANTENNA-RELAY-DESTINATION SELECTION

The solutions of choosing a relay, two SNs, and a transmit antenna are presented in this subsection. Here, a relay and two SNs are selected based on their respective direct channel gains, and TAS is performed through the following three solutions.

1) SINK NODE–HIGH-PRIORITY SN (SHS)

Based on the direct links from the sink node to the SNs in cluster H, SHS intends to jointly select a transmit antenna and an SN in cluster H to maximize the channel gain of the link from the sink node to the selected SN. Thus, the sink node with the chosen transmit antenna and the selected SN in cluster H are given by

$$(S_c, H_c) = \arg \max_{1 \leq p \leq P} \max_{1 \leq n \leq N} \left\{ \left| h_{S_n H_p} \right|^2 \right\}. \quad (1)$$

Furthermore, the best relay and the best SN in cluster L are chosen based on their direct channel gains. Therefore, the chosen relay and SN in cluster L are respectively expressed as

$$R_c = \arg \max_{1 \leq k \leq K} \left\{ \left| h_{S_c R_k} \right|^2 \right\}, \quad (2)$$

and

$$L_c = \arg \max_{1 \leq q \leq Q} \left\{ \left| h_{S_c L_q} \right|^2 \right\}. \quad (3)$$

2) SINK NODE–RELAY (SRS)

Note that the relay will harvest energy from the sink node signal and use that collected energy for its relaying transmission. SRS will focus on jointly selecting a transmit antenna and a relay to maximize the amount of harvested energy at the relay based on the channel gains of the links from the sink node to the relays. Mathematically, the sink node with the chosen transmit antenna and the selected relay in SRS are written as

$$(S_c, R_c) = \arg \max_{1 \leq k \leq K} \max_{1 \leq n \leq N} \left\{ \left| h_{S_n R_k} \right|^2 \right\}. \quad (4)$$

The chosen SN in cluster L in this solution is similar to (3), and the chosen SN in cluster H in SRS is given by

$$H_c = \arg \max_{1 \le p \le P} \left\{ \left| h_{S_c H_p} \right|^2 \right\}. \quad (5)$$

3) SINK NODE–LOW-PRIORITY SN (SLS)

In the considered network, the SNs in cluster H have higher priority than the SNs in cluster L. Therefore, in some specific situations (e.g., the distances from the sink node to the SNs in cluster L are much larger than those from the sink node to the SNs in cluster H), this can cause a reduction in the reception reliability of the SNs in cluster L. SLS is proposed with the aim of improving the performance and reliability of the SNs in cluster L. In particular, SLS jointly selects a transmit antenna and an SN in cluster L for the purpose of providing the maximum channel quality of the link from the sink node to the selected SN in cluster L. Thus, the sink node with the chosen transmit antenna and the selected SN in cluster L in SLS are represented as

$$(S_c, L_c) = \arg \max_{1 \le q \le Q} \max_{1 \le n \le N} \left\{ \left| h_{S_n L_q} \right|^2 \right\}. \quad (6)$$

The chosen relay and SN in cluster H in this solution are similar to (2) and (5), respectively.

B. COOPERATIVE COMMUNICATION PROCESS

As depicted in Fig. 2, the overall cooperative communication process is divided into two phases. According to the PSR protocol, each phase is assumed to have an equal time duration of $T/2$ [21], [22], where T is the block time of the cooperative communication process.

In the first phase, with NOMA, the sink node with the selected transmit antenna S_c broadcasts the superposed message, i.e., $\sqrt{a_{H_c}} x_{H_c} + \sqrt{a_{L_c}} x_{L_c}$, to relay R_c and the selected SNs, i.e., H_c and L_c. Herein, x_{H_c} and x_{L_c} denote the intended transmit signals of SNs H_c and L_c, respectively. a_{H_c} and a_{L_c} $\left(a_{H_c} + a_{L_c} = 1\right)$ are the power allocation coefficients for SNs H_c and L_c, respectively. Since SN H_c has a higher priority than SN L_c, this implies that $a_{H_c} > a_{L_c} > 0$. Thus, the received signal at SN I_c, $I \in \{H, L\}$, is given by

$$y_{S_c I_c} = \left(\sqrt{a_{H_c} P_S} x_{H_c} + \sqrt{a_{L_c} P_S} x_{L_c} \right) h_{S_c I_c} + n_{S_c I_c}, \quad (7)$$

where P_S denotes the transmit power at S_c, $n_{S_c I_c} \sim \mathcal{CN}(0, N_0)$ stands for an additive white Gaussian noise (AWGN) at SN I_c according to the $S_c \rightarrow I_c$ link, and $\mathcal{CN}(0, N_0)$ indicates a scalar complex Gaussian distribution with zero mean and variance N_0. From (7), the instantaneous signal-to-interference-and-noise ratio (SINR) at SN H_c to detect x_{H_c} is written as

$$\gamma_{S_c H_c}^{x_{H_c}} = \frac{a_{H_c} \gamma_S \left| h_{S_c H_c} \right|^2}{a_{L_c} \gamma_S \left| h_{S_c H_c} \right|^2 + 1}, \quad (8)$$

where $\gamma_S = \frac{P_S}{N_0}$ denotes the average transmit SNR.

At SN L_c, with NOMA, it first decodes the message x_{H_c} and then removes this component from its observation to detect its own message (i.e., x_{L_c}) by employing successive interference cancellation (SIC) [30]. This is clear since $a_{H_c} > a_{L_c} > 0$. Thus, based on (7), the SINR and SNR at SN L_c to detect x_{H_c} and x_{L_c} are respectively expressed as

$$\gamma_{S_c L_c}^{x_{H_c}} = \frac{a_{H_c} \gamma_S \left| h_{S_c L_c} \right|^2}{a_{L_c} \gamma_S \left| h_{S_c L_c} \right|^2 + 1}, \quad (9)$$

and

$$\gamma_{S_c L_c}^{x_{L_c}} = a_{L_c} \gamma_S \left| h_{S_c L_c} \right|^2. \quad (10)$$

At relay R_c, with the PSR protocol, it employs a portion of the received power ρP_S $(0 < \rho < 1)$ for energy scavenging and the remaining portion $(1 - \rho) P_S$ for information processing, where ρ denotes the power-splitting ratio. Thus, the harvested energy at relay R_c over time $T/2$ is written as

$$\mathcal{E}_{R_c} = \eta \rho P_S \left| h_{S_c R_c} \right|^2 T/2, \quad (11)$$

where η denotes the energy conversion efficiency.

For information processing, the received signal at relay R_c can be given by

$$y_{S_c R_c} = \sqrt{1 - \rho} \left(\sqrt{a_{H_c} P_S} x_{H_c} + \sqrt{a_{L_c} P_S} x_{L_c} \right) h_{S_c R_c} + n_{S_c R_c}, \quad (12)$$

where $n_{S_c R_c} \sim \mathcal{CN}(0, N_0)$ denotes an AWGN at relay R_c according to the $S_c \rightarrow R_c$ link.

In the second phase, relay R_c forwards information to SNs H_c and L_c by using all energy collected from the signal transmitted by the sink node in the first phase. From (11), the transmit power of relay R_c can be given by

$$P_{R_c} = \frac{\mathcal{E}_{R_c}}{T/2} = b P_S \left| h_{S_c R_c} \right|^2, \quad (13)$$

where $b = \eta \rho$.

Furthermore, relay R_c utilizes either DF or AF to perform relaying transmission.

1) DF PROTOCOL

Relay R_c first decodes the messages x_{H_c} and x_{L_c} received from sink node S_c in (12). After successfully decoding these messages, the relay forwards them to SNs H_c and L_c using NOMA. Specifically, relay R_c first treats x_{L_c} as noise to decode x_{H_c} and then uses SIC to remove this component from its observation before detecting the remaining message, i.e., x_{L_c}. Thus, from (12), the SINR and SNR at relay R_c to detect x_{H_c} and x_{L_c} are respectively given by

$$\gamma_{S_c R_c}^{x_{H_c}} = \frac{(1 - \rho) a_{H_c} \gamma_S \left| h_{S_c R_c} \right|^2}{(1 - \rho) a_{L_c} \gamma_S \left| h_{S_c R_c} \right|^2 + 1}, \quad (14)$$

and

$$\gamma_{S_c R_c}^{x_{L_c}} = (1 - \rho) a_{L_c} \gamma_S \left| h_{S_c R_c} \right|^2. \quad (15)$$

The received signal at SN I_c in this case has the following form:

$$y_{R_c I_c}^{DF} = \left(\sqrt{b_{H_c} P_{R_c}} x_{H_c} + \sqrt{b_{L_c} P_{R_c}} x_{L_c} \right) h_{R_c I_c} + n_{R_c I_c}, \quad (16)$$

where b_{H_c} and b_{L_c} $\left(b_{H_c} > b_{L_c} > 0 \text{ and } b_{H_c} + b_{L_c} = 1\right)$ are the power allocation coefficients for SNs H_c and L_c at relay R_c, respectively, and $n_{R_cI_c} \sim \mathcal{CN}(0, N_0)$ denotes an AWGN at SN I_c according to the $R_c \to I_c$ link.

Therefore, the SINR at SN H_c for detecting x_{H_c} transmitted by relay R_c is expressed as

$$\gamma_{R_cH_c}^{DF,x_{H_c}} = \frac{b_{H_c}P_{R_c}\left|h_{R_cH_c}\right|^2}{b_{L_c}P_{R_c}\left|h_{R_cH_c}\right|^2 + N_0} = \frac{bb_{H_c}\gamma_S\left|h_{S_cR_c}\right|^2\left|h_{R_cH_c}\right|^2}{bb_{L_c}\gamma_S\left|h_{S_cR_c}\right|^2\left|h_{R_cH_c}\right|^2 + 1}, \tag{17}$$

where (17) is obtained by using P_{R_c} in (13).

The SINR and SNR at SN L_c for detecting x_{H_c} and x_{L_c} transmitted by relay R_c are respectively written as

$$\gamma_{R_cL_c}^{DF,x_{H_X}} = \frac{bb_{H_c}\gamma_S\left|h_{S_cR_c}\right|^2\left|h_{R_cL_c}\right|^2}{bb_{L_c}\gamma_S\left|h_{S_cR_c}\right|^2\left|h_{R_cL_c}\right|^2 + 1}, \tag{18}$$

and

$$\gamma_{R_cL_c}^{DF,x_{H_c}} = bb_{L_c}\gamma_S\left|h_{S_cR_c}\right|^2\left|h_{R_cL_c}\right|^2. \tag{19}$$

2) AF PROTOCOL

Relay R_c first amplifies the signal received from sink node S_c in (12) with a power constraint factor $G = \left(P_S\left|h_{S_cR_c}\right|^2 + N_0\right)^{-1/2}$ and then broadcasts the result to SNs H_c and L_c. Therefore, the received signal at SN I_c via the relaying link has the following form:

$$y_{R_cI_c}^{AF} = G\sqrt{(1-\rho)P_SP_{R_c}}\left(\sqrt{a_{H_c}}x_{H_c} + \sqrt{a_{L_c}}x_{L_c}\right) \times h_{S_cR_c}h_{R_cI_c} + GP_{R_c}h_{R_cI_c}n_{S_cR_c} + n_{R_cI_c}, \tag{20}$$

From (20), the SINR at SN H_c for detecting x_{H_c} transmitted by relay R_c is written as in (21) at the bottom of the page, where $a = b(1-\rho)$. The SINR and SNR at SN L_c for detecting x_{H_c} and x_{L_c} transmitted by relay R_c are respectively given by

$$\gamma_{R_cL_c}^{AF,x_{H_c}} = \frac{a\gamma_S^2a_{H_c}\left|h_{S_cR_c}\right|^4\left|h_{R_cL_c}\right|^2}{\left[a\gamma_S^2a_{L_c}\left|h_{S_cR_c}\right|^4\left|h_{R_cL_c}\right|^2 + b\gamma_S\left|h_{S_cR_c}\right|^2\left|h_{R_cL_c}\right|^2 + \gamma_S\left|h_{S_cR_c}\right|^2 + 1\right]}, \tag{22}$$

and

$$\gamma_{R_cL_c}^{AF,x_{L_c}} = \frac{a\gamma_S^2a_{L_c}\left|h_{S_cR_c}\right|^4\left|h_{R_cL_c}\right|^2}{b\gamma_S\left|h_{S_cR_c}\right|^2\left|h_{R_cL_c}\right|^2 + \gamma_S\left|h_{S_cR_c}\right|^2 + 1}, \tag{23}$$

To perform further analyses, we derive the probability density function (PDF) and cumulative distribution function (CDF) of channel power gains, i.e., $\left|h_{S_cR_c}\right|^2$, $\left|h_{S_cH_c}\right|^2$, $\left|h_{S_cL_c}\right|^2$, $\left|h_{R_cH_c}\right|^2$, and $\left|h_{R_cL_c}\right|^2$.

C. DERIVATIONS FOR PDF AND CDF OF CHANNEL POWER GAINS

Let $X = \left|h_{S_cH_c}\right|^2$, $Y = \left|h_{S_CL_c}\right|^2$, $Z = \left|h_{S_cR_c}\right|^2$, $Z_H = \left|h_{R_cH_c}\right|^2$, and $Z_L = \left|h_{R_cL_c}\right|^2$. The CDFs of $V \in \{X, Y, Z\}$ and $W \in \{Z_H, Z_L\}$ are expressed through *Lemma 1* and *Lemma 2*, respectively, as follows:

Lemma 1: Under Nakagami-m fading, the CDF of random variable (RV) $V \in \{X, Y, Z\}$ is given by

$$F_V(x) = \sum_{i=0}^{\chi_V}\sum_{U_A=i}\hat{\Psi}_A^{(\chi_V)}x^{\varphi_A}e^{-\frac{im_{SA}x}{\lambda_{SA}}}, \tag{24}$$

where $U_A = \sum_{j=0}^{m_{SA}-1}u_{A,j}$, $\varphi_A = \sum_{j=0}^{m_{SA}-1}ju_{A,j}$, $\lambda_{SA} = \frac{\Omega_{SA}}{d_{SA}^{\theta_{SA}}}$, and d_{SA} and θ_{SA} denote the distance and path loss exponent of the link from the sink node to the relay or SNs, respectively. Additionally, $\hat{\Psi}_A^{(\chi_V)}$, A, and χ_v are respectively defined as

$$\hat{\Psi}_A^{(\chi_V)} = \binom{\chi_V}{i}(-1)^i\Lambda_A\left[\prod_{j=0}^{m_{SA}-1}\left(\frac{m_{SA}^j}{j!\lambda_{SA}^j}\right)^{u_{A,j}}\right], \tag{25}$$

$$A = \begin{cases} H, & \text{if } V = X \\ L, & \text{if } V = Y \\ R, & \text{if } V = Z, \end{cases} \tag{26}$$

and

$$\chi_V = \begin{cases} \chi_{V,H}, & \text{for SHS} \\ \chi_{V,R}, & \text{for SRS} \\ \chi_{V,L}, & \text{for SLS}, \end{cases} \tag{27}$$

where

$$\chi_{V,H} = \begin{cases} NP, & \text{if } V = X \\ Q, & \text{if } V = Y \\ K, & \text{if } V = Z, \end{cases}$$

$$\chi_{V,R} = \begin{cases} P, & \text{if } V = X \\ Q, & \text{if } V = Y \\ NK, & \text{if } V = Z, \end{cases}$$

$$\chi_{V,L} = \begin{cases} P, & \text{if } V = X \\ NQ, & \text{if } V = Y \\ K, & \text{if } V = Z, \end{cases}$$

$$\gamma_{R_cH_c}^{AF,x_{H_c}} = \frac{G^2(1-\rho)P_SP_{R_c}a_{H_c}\left|h_{S_cR_c}\right|^2\left|h_{R_cH_c}\right|^2}{G^2(1-\rho)P_SP_{R_c}a_{L_c}\left|h_{S_cR_c}\right|^2\left|h_{R_cH_c}\right|^2 + G^2P_{R_c}\left|h_{R_cH_c}\right|^2N_0 + N_0} = \frac{a\gamma_S^2a_{H_c}\left|h_{S_cR_c}\right|^4\left|h_{R_cH_c}\right|^2}{a\gamma_S^2a_{L_c}\left|h_{S_cR_c}\right|^4\left|h_{R_cH_c}\right|^2 + b\gamma_S\left|h_{S_cR_c}\right|^2\left|h_{R_cH_c}\right|^2 + \gamma_S\left|h_{S_cR_c}\right|^2 + 1}, \tag{21}$$

and

$$\Lambda_A = \binom{i}{u_{A,0}, \ldots, u_{A,m_{SA}-1}}.$$

Proof: See Appendix A. ■

From *Lemma 1*, the PDF of RV V is obtained as

$$\begin{aligned} f_V(x) &= \frac{dF_V(x)}{dx} \\ &= \frac{\chi_V m_{SA}^{m_{SA}}}{\Gamma(m_{SA})\lambda_{SA}^{m_{SA}}} \sum_{i=0}^{\chi_V-1} \sum_{U_A=i} \Psi_A^{(\chi_V)} x^{\varphi_A+m_{SA}-1} \\ &\quad \times e^{-\frac{(i+1)m_{SA}x}{\lambda_{SA}}}, \end{aligned} \tag{28}$$

where $\Psi_A^{(\chi_V)}$ is defined as

$$\Psi_A^{(\chi_V)} = \binom{\chi_V - 1}{i} \Lambda_A (-1)^i \prod_{j=0}^{m_{SA}-1} \left(\frac{m_{SA}^j}{j!\lambda_{SA}^j}\right)^{u_{A,j}}. \tag{29}$$

Lemma 2: Under Nakagami-m fading, the CDF of RV $W \in \{Z_H, Z_L\}$ is given by

$$F_W(x) = 1 - \sum_{i=0}^{m_{RB}-1} \frac{m_{RB}^i}{i!\lambda_{RB}^i} x^i e^{-\frac{m_{RB}x}{\lambda_{RB}}}, \tag{30}$$

where $\lambda_{RB} = \frac{\Omega_{RB}}{d_{RB}^{\theta_{RB}}}$, and d_{RB} and θ_{RB} denote the distance and path loss exponent of the link from the relay to the SNs. Additionally, B is given by

$$B = \begin{cases} H, & \text{if } W = Z_H \\ L, & \text{if } W = Z_L. \end{cases} \tag{31}$$

Proof: See Appendix B. ■

IV. PERFORMANCE ANALYSIS WITH DF RELAYING STRATEGY

In this section, the performance analysis in terms of the OP of SNs H_c and L_c is presented, where the DF relaying strategy is considered. Let r_H and r_L denote the target data rates of SNs H_c and L_c, respectively.

A. AT HIGH-PRIORITY SN H_c

The OP of SN H_c with DF relaying is given by

$$\mathcal{O}_H^{DF} = \Pr\{E_{H,1}\}\left(\Pr\{E_R\} + \Pr\{\bar{E}_R, E_{H,2}\}\right), \tag{32}$$

where $E_{H,1}$ and $E_{H,2}$ denote the events in which SN H_c unsuccessfully decodes the message x_{H_c} received from the sink node S_c and relay R_c, respectively. Moreover, E_R is the event where relay R_c unsuccessfully decodes the message x_{H_c} or x_{L_c} received from sink node S_c, and $\bar{E}_R$ is the complementary event of E_R. In more detail, $\Pr\{E_{H,1}\}$ is represented as

$$\begin{aligned} \Pr\{E_{H,1}\} &= \Pr\left\{\gamma_{S_cH_c}^{x_{H_c}} < \gamma_H\right\} \\ &= \Pr\left\{\frac{a_{H_c}\gamma_S X}{a_{L_c}\gamma_S X + 1} < \gamma_H\right\} \\ &= \Pr\left[\left(a_{H_c} - a_{L_c}\gamma_H\right)\gamma_S X < \gamma_H\right] \\ &= \begin{cases} 1, & \gamma_H \geq \beta \\ F_X\left(\frac{g_H}{\gamma_S}\right), & \gamma_H < \beta, \end{cases} \end{aligned} \tag{33}$$

where $\gamma_H = 2^{2r_H} - 1$ is the SNR threshold for correctly decoding the message x_{H_c}, $\beta = \frac{a_{H_c}}{a_{L_c}}$, and $g_H = \frac{\gamma_H}{a_{H_c} - a_{L_c}\gamma_H}$.

Furthermore, $\Pr\{E_R\}$ is given by

$$\begin{aligned} \Pr\{E_R\} &= 1 - \Pr\left\{\gamma_{S_cR_c}^{x_{H_c}} \geq \gamma_H, \gamma_{S_cR_c}^{x_{L_c}} \geq \gamma_L\right\} \\ &= 1 - \Pr\left\{\frac{(1-\rho)a_{H_c}\gamma_S Z}{(1-\rho)a_{L_c}\gamma_S Z + 1} \geq \gamma_H, \right. \\ &\qquad \left. (1-\rho)a_{L_c}\gamma_S Z \geq \gamma_L\right\} \\ &= \begin{cases} 1, & \gamma_H \geq \beta \\ 1 - \Pr\left\{Z \geq \frac{g_H}{(1-\rho)\gamma_S}, \right. \\ \qquad \left. Z \geq \frac{\gamma_L}{(1-\rho)a_{L_c}\gamma_S}\right\}, & \gamma_H < \beta \end{cases} \\ &= \begin{cases} 1, & \gamma_H \geq \beta \\ F_Z(\omega_R), & \gamma_H < \beta, \end{cases} \end{aligned} \tag{34}$$

where $\gamma_L = 2^{2r_L} - 1$ is the SNR threshold for correctly decoding the message x_{L_c}, $\omega_R = \frac{\omega_{HL}}{(1-\rho)}$, and $\omega_{HL} = \frac{1}{\gamma_S}\max\left\{g_H, \frac{\gamma_L}{a_{L_c}}\right\}$.

$\Pr\{\bar{E}_R, E_{H,2}\}$ has the following form:

$$\begin{aligned} &\Pr\{\bar{E}_R, E_{H,2}\} \\ &= \Pr\left\{\gamma_{S_cR_c}^{x_{H_c}} \geq \gamma_H, \gamma_{S_cR_c}^{x_{L_c}} \geq \gamma_L, \gamma_{R_cH_c}^{DF,x_{H_c}} < \gamma_H\right\} \\ &= \Pr\left\{\frac{(1-\rho)a_{H_c}\gamma_S Z}{(1-\rho)a_{L_x}\gamma_S Z + 1} \geq \gamma_H, \right. \\ &\qquad \left. (1-\rho)a_{L_c}\gamma_S Z \geq \gamma_L, \frac{bb_{H_c}\gamma_S Z Z_H}{bb_{L_c}\gamma_S Z Z_H + 1} < \gamma_H\right\} \\ &= \begin{cases} 0, & \gamma_H \geq \beta \\ 1 - F_Z(\omega_R), & \hat{\beta} \leq \gamma_H < \beta \\ \underbrace{\Pr\left\{Z \geq \omega_R, Z_H < \frac{\hat{g}_H}{b\gamma_S Z}\right\}}_{\Theta_{H,1}^{DF}}, & \gamma_H < \min\left(\beta, \hat{\beta}\right), \end{cases} \end{aligned} \tag{35}$$

where $\hat{\beta} = \frac{b_{H_c}}{b_{L_c}}$, $\hat{g}_H = \frac{\gamma_H}{b_{H_c} - b_{L_c}\gamma_H}$, and $\Theta_{H,1}^{DF}$ is expressed as

$$\begin{aligned} \Theta_{H,1}^{DF} &= \int_{\omega_R}^{\infty} F_{Z_H}\left(\frac{\hat{g}_H}{b\gamma_S x}\right) f_Z(x)\, dx \\ &= 1 - F_Z(\omega_R) - \frac{\chi_Z m_{SR}^{m_{SR}}}{\Gamma(m_{SR})\lambda_{SR}^{m_{SR}}} \sum_{i=0}^{\chi_Z-1} \sum_{U_R=i} \sum_{j=0}^{m_{RH}-1} \\ &\quad \times \frac{\Psi_R^{(\chi_Z)} m_{RH}^j}{j!\lambda_{RH}^j} \left(\frac{\hat{g}_H}{b\gamma_S}\right)^j \\ &\quad \times \underbrace{\int_{\omega_R}^{\infty} x^{\varphi_R + m_{SR} - j - 1} e^{-\frac{m_{RH}\hat{g}_H}{b\gamma_S\lambda_{RH}x} - \frac{(i+1)m_{SR}x}{\lambda_{SR}}} dx}_{\mathcal{I}}. \end{aligned} \tag{36}$$

To derive the integral $\mathcal{I}$ in (36), we first use the series representation of the exponential function in [49, eq. (1.211)]

for the term $e^{-\frac{m_{RH}\hat{g}_H}{b\gamma_S\lambda_{RH}x}}$, and then we apply [49, eq. (3.381.3)]. Specifically, it is given by

$$\mathcal{I} = \sum_{r=0}^{\infty} \frac{(-1)^r}{r!} \left(\frac{m_{RH}\hat{g}_H}{b\gamma_S\lambda_{RH}}\right)^r \left[\frac{\lambda_{SR}}{(i+1)\,m_{SR}}\right]^{\phi} \times \Gamma\left[\phi, \frac{(i+1)\,m_{SR}\omega_R}{\lambda_{SR}}\right], \quad (37)$$

where $\phi = \varphi_R + m_{SR} - j - r$. Thus, $\Theta_{H,1}^{DF}$ in (36) is rewritten as

$$\Theta_{H,1}^{DF} = 1 - F_Z(\omega_R) - \Theta_{H,2}^{DF}, \quad (38)$$

where

$$\Theta_{H,2}^{DF} = \widetilde{\sum}_{H,DF}^{(\chi_Z)} \hat{\Theta}_R^{(\chi_Z)} \left(\frac{m_{RH}\hat{g}_H}{\lambda_{RH}}\right)^{j+r},$$

$$\widetilde{\sum}_{H,DF}^{(\chi_Z)} = \sum_{i=0}^{\chi_Z-1} \sum_{U_R=i} \sum_{j=0}^{m_{RH}-1} \sum_{r=0}^{\infty},$$

and

$$\hat{\Theta}_R^{(\chi_Z)} = \frac{(-1)^r}{j!r!} \frac{\Psi_R^{(\chi_Z)} \chi_Z m_{SR}^{m_{SR}}}{\Gamma(m_{SR})\,\lambda_{SR}^{m_{SR}}} \left(\frac{1}{b\gamma_S}\right)^{j+r} \times \left[\frac{\lambda_{SR}}{(i+1)\,m_{SR}}\right]^{\phi} \Gamma\left[\phi, \frac{(i+1)\,m_{SR}\omega_R}{\lambda_{SR}}\right].$$

Finally, substituting (33), (34), and (35) into (32), $\mathcal{O}_H^{DF}$ is given by

$$\mathcal{O}_H^{DF} = \begin{cases} 1, & \gamma_H \geq \beta \\ F_X\left(\frac{g_H}{\gamma_S}\right), & \hat{\beta} \leq \gamma_H < \beta \\ F_X\left(\frac{g_H}{\gamma_S}\right)\left(1 - \Theta_{H,2}^{DF}\right), & \gamma_H < \min\left(\beta, \hat{\beta}\right). \end{cases} \quad (39)$$

Next, we will consider $\mathcal{O}_H^{DF}$ in the case of using different antenna-relay-destination selection strategies, i.e., SHS, SRS, and SLS.

1) FOR SHS

From (39), the OP of SN H_c is written as

$$\mathcal{O}_H^{DF,SHS} = \begin{cases} 1, & \gamma_H \geq \beta \\ F_X^{SHS}\left(\frac{g_H}{\gamma_S}\right), & \hat{\beta} \leq \gamma_H < \beta \\ F_X^{SHS}\left(\frac{g_H}{\gamma_S}\right)\left(1 - \Theta_{H,2}^{DF,SHS}\right), & \gamma_H < \min\left(\beta, \hat{\beta}\right), \end{cases} \quad (40)$$

where $F_X^{SHS}(x)$ and $\Theta_{H,2}^{DF,SHS}$ are obtained by using (24) for SHS. Specifically, they are given by

$$F_X^{SHS}(x) = \sum_{i=0}^{NP} \sum_{U_H=i} \hat{\Psi}_H^{(NP)} x^{\varphi_H} e^{-\frac{im_{SH}x}{\lambda_{SH}}}, \quad (41)$$

and

$$\Theta_{H,2}^{DF,SHS} = \widetilde{\sum}_{H,DF}^{(K)} \hat{\Theta}_R^{(K)} \left(\frac{m_{RH}\hat{g}_H}{\lambda_{RH}}\right)^{j+r}. \quad (42)$$

2) FOR SRS

The OP of SN H_c in this case has the following form:

$$\mathcal{O}_H^{DF,SRS} = \begin{cases} 1, & \gamma_H \geq \beta \\ F_X^{SRS}\left(\frac{g_H}{\gamma_S}\right), & \hat{\beta} \leq \gamma_H < \beta \\ F_X^{SRS}\left(\frac{g_H}{\gamma_S}\right)\left(1 - \Theta_{H,2}^{DF,SRS}\right), & \gamma_H < \min\left(\beta, \hat{\beta}\right), \end{cases} \quad (43)$$

where $F_X^{SRS}(x)$ and $\Theta_{H,2}^{DF,SRS}$ are derived by using (24) for SRS as follows:

$$F_X^{SRS}(x) = \sum_{i=0}^{P} \sum_{U_H=i} \hat{\Psi}_H^{(P)} x^{\varphi_H} e^{-\frac{im_{SH}x}{\lambda_{SH}}}, \quad (44)$$

and

$$\Theta_{H,2}^{DF,SRS} = \widetilde{\sum}_{H,DF}^{(NK)} \hat{\Theta}_R^{(NK)} \left(\frac{m_{RH}\hat{g}_H}{\lambda_{RH}}\right)^{j+r}. \quad (45)$$

3) FOR SLS

The OP of SN H_c in this case is given by

$$\mathcal{O}_H^{DF,SLS} = \begin{cases} 1, & \gamma_H \geq \beta \\ F_X^{SLS}\left(\frac{g_H}{\gamma_S}\right), & \hat{\beta} \leq \gamma_H < \beta \\ F_X^{SLS}\left(\frac{g_H}{\gamma_S}\right)\left(1 - \Theta_{H,2}^{DF,SLS}\right), & \gamma_H < \min\left(\beta, \hat{\beta}\right), \end{cases} \quad (46)$$

where $F_X^{SLS}(x) = F_X^{SRS}(x)$ and $\Theta_{H,2}^{DF,SLS} = \Theta_{H,2}^{DF,SHS}$.

B. AT LOW-PRIORITY SN L_c

The OP of SN L_c in this case is given by

$$\mathcal{O}_L^{DF} = \Pr\left\{E_{L,1}\right\}\left(\Pr\left\{E_R\right\} + \Pr\left\{\bar{E}_R, E_{L,2}\right\}\right), \quad (47)$$

where $E_{L,1}$ and $E_{L,2}$ denote the events in which SN L_c unsuccessfully decodes either x_{H_c} or x_{L_c} received from sink node S_c and relay R_c, respectively. Specifically, the derivation of $\Pr\{E_R\}$ is shown in (34). Additionally, $\Pr\left\{E_{L,1}\right\}$ and $\Pr\left\{\bar{E}_R, E_{L,2}\right\}$ are respectively represented as

$$\begin{aligned} \Pr\left\{E_{L,1}\right\} &= 1 - \Pr\left\{\gamma_{S_cL_c}^{x_{H_c}} \geq \gamma_H, \gamma_{S_cL_c}^{x_{L_c}} \geq \gamma_L\right\} \\ &= \Pr\left\{\frac{a_{H_c}\gamma_S Y}{a_{L_c}\gamma_S Y + 1} \geq \gamma_H, a_{L_c}\gamma_S Y \geq \gamma_L\right\} \\ &= \begin{cases} 1, & \gamma_H \geq \beta \\ F_Y(\omega_{HL}), & \gamma_H < \beta, \end{cases} \end{aligned} \quad (48)$$

and

$$\begin{aligned}
&\Pr\left\{\bar{E}_R, E_{L,2}\right\} \\
&= \Pr\left\{\gamma_{S_cR_c}^{x_{H_c}} \geq \gamma_H, \gamma_{S_cR_c}^{x_{L_c}} \geq \gamma_L, \gamma_{R_cL_c}^{DF,x_{H_c}} < \gamma_H\right\} \\
&\quad + \Pr\left\{\gamma_{S_cR_c}^{x_{H_c}} \geq \gamma_H, \gamma_{S_cR_c}^{x_{L_c}} \geq \gamma_L, \gamma_{R_cL_c}^{DF,x_{H_c}} \geq \gamma_H, \right. \\
&\qquad \left. \gamma_{R_cL_c}^{DF,x_{L_c}} < \gamma_L\right\} \\
&= \Theta_{L,1}^{DF} + \Theta_{L,2}^{DF}. \qquad (49)
\end{aligned}$$

After some algebraic manipulations similar to the derivation for $\Theta_{H,1}^{DF}$ in (35), $\Theta_{L,1}^{DF}$ in (49) is written as

$$\Theta_{L,1}^{DF} = \begin{cases} 0, & \gamma_H \geq \beta \\ 1 - F_Z(\omega_R), & \hat{\beta} \leq \gamma_H < \beta \\ \Theta_{L,11}^{DF}, & \gamma_H < \min\left(\beta, \hat{\beta}\right), \end{cases} \qquad (50)$$

where

$$\begin{aligned}
\Theta_{L,11}^{DF} &= \Pr\left\{Z \geq \omega_R, Z_L < \frac{\hat{g}_H}{b\gamma_S Z}\right\} \\
&= 1 - F_Z(\omega_R) - \Theta_{L,12}^{DF}, \\
\Theta_{L,12}^{DF} &= \widetilde{\sum}_{L,DF}^{(\chi_Z)} \hat{\Theta}_R^{(\chi_Z)} \left(\frac{m_{RL}\hat{g}_H}{\lambda_{RL}}\right)^{j+r},
\end{aligned}$$

and

$$\widetilde{\sum}_{L,DF}^{(\chi_Z)} = \sum_{i=0}^{\chi_Z - 1} \sum_{U_R=i} \sum_{j=0}^{m_{RL}-1} \sum_{r=0}^{\infty}.$$

$\Theta_{L,2}^{DF}$ in (49) is given by

$$\Theta_{L,2}^{DF} = \begin{cases} 0, & \gamma_H \geq \beta \\ 0, & \hat{\beta} \leq \gamma_H < \beta \\ \Theta_{L,21}^{DF}, & \gamma_H < \min\left(\beta, \hat{\beta}\right), \end{cases} \qquad (51)$$

where

$$\begin{aligned}
\Theta_{L,21}^{DF} &= \Pr\left\{Z \geq \omega_R, Z_L \geq \frac{\hat{g}_H}{b\gamma_S Z}, Z_L < \frac{\gamma_L}{bb_{L_c}\gamma_S Z}\right\} \\
&= \begin{cases} 0, & \gamma_L < b_{L_c}\hat{g}_H \\ \Theta_{L,22}^{DF}, & \gamma_L \geq b_{L_c}\hat{g}_H, \end{cases} \\
\Theta_{L,22}^{DF} &= \Pr\left\{Z \geq \omega_R, \frac{\hat{g}_H}{b\gamma_S Z} \leq Z_L < \frac{\gamma_L}{bb_{L_c}\gamma_S Z}\right\} \\
&= \int_{\omega_R}^{\infty} \left[F_{Z_L}\left(\frac{\gamma_L}{bb_{L_c}\gamma_S x}\right) - F_{Z_L}\left(\frac{\hat{g}_H}{b\gamma_S x}\right)\right] f_Z(x)\, dx \\
&= \Theta_{L,12}^{DF} - \Theta_{L,23}^{DF},
\end{aligned}$$

and

$$\Theta_{L,23}^{DF} = \widetilde{\sum}_{L,DF}^{(\chi_Z)} \hat{\Theta}_R^{(\chi_Z)} \left(\frac{m_{RL}\gamma_L}{b_{L_c}\lambda_{RL}}\right)^{j+r}.$$

Finally, by substituting (48), (34), and (49) into (47), $\mathcal{O}_L^{DF}$ is obtained as

$$\mathcal{O}_L^{DF} = \begin{cases} 1, & \gamma_H \geq \beta \\ F_Y(\omega_{HL}), & \hat{\beta} \leq \gamma_H < \beta \\ \Theta_L^{DF}, & \gamma_H < \min\left(\beta, \hat{\beta}\right), \end{cases} \qquad (52)$$

where Θ_L^{DF} is defined as

$$\Theta_L^{DF} = \begin{cases} F_Y(\omega_{HL})\left(1 - \Theta_{L,12}^{DF}\right), & \gamma_L < b_{L_c}\hat{g}_H \\ F_Y(\omega_{HL})\left(1 - \Theta_{L,23}^{DF}\right), & \gamma_L \geq b_{L_c}\hat{g}_H. \end{cases} \qquad (53)$$

1) FOR SHS

From (52), the OP of SN L_c in this case is written as

$$\mathcal{O}_L^{DF,SHS} = \begin{cases} 1, & \gamma_H \geq \beta \\ F_Y^{SHS}(\omega_{HL}), & \hat{\beta} \leq \gamma_H < \beta \\ \Theta_L^{DF,SHS}, & \gamma_H < \min\left(\beta, \hat{\beta}\right), \end{cases} \qquad (54)$$

where

$$\Theta_L^{DF,SHS} = \begin{cases} F_Y^{SHS}(\omega_{HL})\left(1 - \Theta_{L,12}^{DF,SHS}\right), & \gamma_L < b_{L_c}\hat{g}_H \\ F_Y^{SHS}(\omega_{HL})\left(1 - \Theta_{L,23}^{DF,SHS}\right), & \gamma_L \geq b_{L_c}\hat{g}_H, \end{cases}$$

$F_Y^{SHS}(x)$, $\Theta_{L,12}^{DF,SHS}$, and $\Theta_{L,23}^{DF,SHS}$ are obtained by using (24) for SHS, i.e.,

$$F_Y^{SHS}(x) = \sum_{i=0}^{Q} \sum_{U_L=i} \hat{\Psi}_L^{(Q)} x^{\varphi_L} e^{-\frac{im_{SL}x}{\lambda_{SL}}}, \qquad (55)$$

$$\Theta_{L,12}^{DF,SHS} = \widetilde{\sum}_{L,DF}^{(K)} \hat{\Theta}_R^{(K)} \left(\frac{m_{RL}\hat{g}_H}{\lambda_{RL}}\right)^{j+r}, \qquad (56)$$

and

$$\Theta_{L,23}^{DF,SHS} = \widetilde{\sum}_{L,DF}^{(K)} \hat{\Theta}_R^{(K)} \left(\frac{m_{RL}\gamma_L}{b_{L_c}\lambda_{RL}}\right)^{j+r}. \qquad (57)$$

2) FOR SRS

The OP of SN L_c in this case is expressed as

$$\mathcal{O}_L^{DF,SRS} = \begin{cases} 1, & \gamma_H \geq \beta \\ F_Y^{SRS}(\omega_{HL}), & \hat{\beta} \leq \gamma_H < \beta \\ \Theta_L^{DF,SRS}, & \gamma_H < \min\left(\beta, \hat{\beta}\right), \end{cases} \qquad (58)$$

where

$$\Theta_L^{DF,SRS} = \begin{cases} F_Y^{SRS}(\omega_{HL})\left(1 - \Theta_{L,12}^{DF,SRS}\right), & \gamma_L < b_{L_c}\hat{g}_H \\ F_Y^{SRS}(\omega_{HL})\left(1 - \Theta_{L,23}^{DF,SRS}\right), & \gamma_L \geq b_{L_c}\hat{g}_H, \end{cases}$$

$F_Y^{SRS}(x) = F_Y^{SHS}(x)$, $\Theta_{L,12}^{DF,SRS}$ and $\Theta_{L,23}^{DF,SRS}$ are derived by using (24) for SRS as follows:

$$\Theta_{L,12}^{DF,SRS} = \widetilde{\sum}_{L,DF}^{(NK)} \hat{\Theta}_R^{(NK)} \left(\frac{m_{RL}\hat{g}_H}{\lambda_{RL}}\right)^{j+r}, \qquad (59)$$

and

$$\Theta_{L,23}^{DF,SRS} = \widetilde{\sum}_{L,DF}^{(NK)} \hat{\Theta}_R^{(NK)} \left(\frac{m_{RL}\gamma_L}{b_{L_c}\lambda_{RL}}\right)^{j+r}. \qquad (60)$$

3) FOR SLS

The OP of SN L_c in this case has the following form:

$$\mathcal{O}_L^{DF,SLS} = \begin{cases} 1, & \gamma_H \geq \beta \\ F_Y^{SLS}(\omega_{HL}), & \hat{\beta} \leq \gamma_H < \beta \\ \Theta_L^{DF,SLS}, & \gamma_H < \min\left(\beta, \hat{\beta}\right), \end{cases} \quad (61)$$

where

$$\Theta_L^{DF,SLS} = \begin{cases} F_Y^{SLS}(\omega_{HL})\left(1 - \Theta_{L,12}^{DF,SLS}\right), & \gamma_L < b_{L_c}\hat{g}_H \\ F_Y^{SLS}(\omega_{HL})\left(1 - \Theta_{L,23}^{DF,SLS}\right), & \gamma_L \geq b_{L_c}\hat{g}_H, \end{cases}$$

$\Theta_{L,12}^{DF,SLS} = \Theta_{L,12}^{DF,SHS}$, $\Theta_{L,23}^{DF,SLS} = \Theta_{L,23}^{DF,SHS}$, and $F_Y^{SLS}(x)$ is given by

$$F_Y^{SLS}(x) = \sum_{i=0}^{NQ} \sum_{U_L=i} \hat{\Psi}_L^{(NQ)} x^{\varphi_L} e^{-\frac{im_{SL}x}{\lambda_{SL}}}. \quad (62)$$

V. PERFORMANCE ANALYSIS WITH AF RELAYING STRATEGY

In this section, the performance analysis in terms of the OP of SNs H_c and L_c is presented, where the AF relaying strategy is considered.

A. AT HIGH-PRIORITY SN H_c

The OP of SN H_c in this case is expressed as

$$\begin{aligned} \mathcal{O}_H^{AF} &= \Pr\left\{\gamma_{S_cH_c}^{x_{H_c}} < \gamma_H, \gamma_{R_cH_c}^{AF,x_{H_c}} < \gamma_H\right\} \\ &= \underbrace{\Pr\left\{\gamma_{S_cH_c}^{x_{H_c}} < \gamma_H\right\}}_{\Theta_{H,1}^{AF}} \underbrace{\Pr\left\{\gamma_{R_cH_c}^{AF,x_{H_c}} < \gamma_H\right\}}_{\Theta_{H,2}^{AF}}, \end{aligned} \quad (63)$$

where $\Theta_{H,1}^{AF}$ is calculated as

$$\begin{aligned} \Theta_{H,1}^{AF} &= \Pr\{E_{H,1}\} \\ &= \begin{cases} 1, & \gamma_H \geq \beta \\ F_X\left(\frac{g_H}{\gamma_S}\right), & \gamma_H < \beta. \end{cases} \end{aligned} \quad (64)$$

To derive $\Theta_{H,2}^{AF}$ in (63), we expand it by using (21) as follows:

$$\Theta_{H,2}^{AF} = \Pr\left\{\frac{a\gamma_S^2 a_{H_c} Z^2 Z_H}{a\gamma_S^2 a_{L_c} Z^2 Z_H + b\gamma_S Z Z_H + \gamma_S Z + 1} < \gamma_H\right\}. \quad (65)$$

Note that directly deriving (65) is challenging; thus, an approximation solution is used to obtain the closed-form expression of $\Theta_{H,2}^{AF}$. Specifically, as used in [12], [13], and [21], in a high SNR regime (where the transmit power is much larger than the noise power, i.e., $\gamma_S \gg 1$), (65) is approximated as

$$\begin{aligned} \Theta_{H,2}^{AF} &\approx \Pr\left\{\frac{a\gamma_S a_{H_c} Z Z_H}{a\gamma_S a_{L_c} Z Z_H + bZ_H + 1} < \gamma_H\right\} \\ &= \Pr\{Z \leq \delta\} + \Pr\left\{Z_H < \frac{\delta}{b(x-\delta)}, Z > \delta\right\} \\ &= \int_0^{\delta} f_Z(x)\,dx + \int_{\delta}^{\infty} F_{Z_H}\left(\frac{\delta}{b(x-\delta)}\right) f_Z(x)\,dx, \end{aligned} \quad (66)$$

where $\delta = \frac{bg_H}{a\gamma_S}$. By substituting (28) with $V = Z$ and (30) with $W = Z_H$ into (66), $\Theta_{H,2}^{AF}$ is rewritten as

$$\begin{aligned} \Theta_{H,2}^{AF} = 1 - \frac{\chi_Z m_{SR}^{m_{SR}}}{\Gamma(m_{SR})\lambda_{SR}^{m_{SR}}} \sum_{i=0}^{\chi_Z - 1} \sum_{U_R=i} \sum_{r=0}^{m_{RH}-1} \frac{m_{RH}^r \Psi_R^{(\chi_Z)} \delta^r}{r! \lambda_{RH}^r b^r} \\ \times \int_{\delta}^{\infty} \frac{x^{\varphi_R + m_{SR} - 1}}{(x-\delta)^r} e^{-\frac{m_{RH}\delta}{b\lambda_{RH}(x-\delta)} - \frac{(i+1)m_R x}{\lambda_{SR}}} dx. \end{aligned} \quad (67)$$

Based on (67), after changing variable $t = x - \delta$ and then applying [49, eq. (3.471.9)], $\Theta_{H,2}^{AF}$ is finally given by

$$\Theta_{H,2}^{AF} = 1 - \widetilde{\sum}_{H,AF}^{(\chi_Z)} \Theta_{R,\delta}^{(\chi_Z)} \left(\frac{m_{RH}}{b\lambda_{RH}}\right)^{\frac{s+r+1}{2}}, \quad (68)$$

where

$$\begin{aligned} \widetilde{\sum}_{H,AF}^{(\chi_Z)} &= \sum_{i=0}^{\chi_Z - 1} \sum_{U_R=i} \sum_{r=0}^{m_{RH}-1} \sum_{s=0}^{\varphi_R + m_{SR} - 1}, \\ \Theta_{R,\delta}^{(\chi_Z)} &= \frac{2\Psi_R^{(\chi_Z)} \chi_Z m_{SR}^{m_{SR}}}{r!\Gamma(m_{SR})\lambda_{SR}^{m_{SR}}} \binom{\varphi_R + m_{SR} - 1}{s} \delta^{\frac{c_1}{2}} \\ &\quad \times \left[\frac{\lambda_{SR}}{(i+1)m_{SR}}\right]^{\frac{s-r+1}{2}} e^{-\frac{(i+1)m_{SR}\delta}{\lambda_{SR}}} \\ &\quad \times \mathcal{K}_{s-r+1}\left[2\sqrt{\frac{(i+1)\delta m_{SR} m_{RH}}{b\lambda_{SR}\lambda_{RH}}}\right], \\ c_1 &= 2\varphi_R + 2m_{SR} + r - s - 1, \end{aligned}$$

and $\mathcal{K}_v(\cdot)$ stands for the v^{th}-order modified Bessel function of the second kind.

Finally, by substituting (64) and (68) into (63), $\mathcal{O}_H^{AF}$ is obtained as

$$\mathcal{O}_H^{AF} = \begin{cases} \Theta_{H,2}^{AF}, & \gamma_H \geq \beta \\ F_X\left(\frac{g_H}{\gamma_S}\right)\Theta_{H,2}^{AF}, & \gamma_H < \beta. \end{cases} \quad (69)$$

1) FOR SHS

Based on (69), the OP of SN H_c in this case is written as

$$\mathcal{O}_H^{AF,SHS} = \begin{cases} \Theta_{H,2}^{AF,SHS}, & \gamma_H \geq \beta \\ F_X^{SHS}\left(\frac{g_H}{\gamma_S}\right)\Theta_{H,2}^{AF,SHS}, & \gamma_H < \beta, \end{cases} \quad (70)$$

where $F_X^{SHS}(x)$ is shown in (41) and $\Theta_{H,2}^{AF,SHS}$ is given by

$$\Theta_{H,2}^{AF,SHS} = 1 - \widetilde{\sum}_{H,AF}^{(K)} \Theta_{R,\delta}^{(K)} \left(\frac{m_{RH}}{b\lambda_{RH}}\right)^{\frac{s+r+1}{2}}. \quad (71)$$

2) FOR SRS

With SRS, the OP of SN H_c is given by

$$\mathcal{O}_H^{AF,SRS} = \begin{cases} \Theta_{H,2}^{AF,SRS}, & \gamma_H \geq \beta \\ F_X^{SRS}\left(\frac{g_H}{\gamma_S}\right)\Theta_{H,2}^{AF,SRS}, & \gamma_H < \beta, \end{cases} \quad (72)$$

where $F_X^{SRS}(x)$ is obtained in (44) and $\Theta_{H,2}^{AF,SRS}$ is expressed as

$$\Theta_{H,2}^{AF,SRS} = 1 - \widetilde{\sum}_{H,AF}^{(NK)} \Theta_{R,\delta}^{(NK)} \left(\frac{m_{RH}}{b\lambda_{RH}}\right)^{\frac{s+r+1}{2}}. \quad (73)$$

3) FOR SLS

In this case, the OP of SN H_c has the following form:

$$\mathcal{O}_H^{AF,SLS} = \begin{cases} \Theta_{H,2}^{AF,SLS}, & \gamma_H \geq \beta \\ F_X^{SLS}\left(\frac{g_H}{\gamma_S}\right)\Theta_{H,2}^{AF,SLS}, & \gamma_H < \beta, \end{cases} \quad (74)$$

where $\Theta_{H,2}^{AF,SLS} = \Theta_{H,2}^{AF,SHS}$ and $F_X^{SLS}(x)$ are similar to $F_X^{SRS}(x)$ in (44).

B. AT LOW-PRIORITY SN L_c

The OP of SN L_c in this case is expressed as

$$\begin{aligned} \mathcal{O}_L^{AF} &= \left(1 - \Pr\left\{\gamma_{S_cL_c}^{x_{H_c}} \geq \gamma_H, \gamma_{S_cL_c}^{x_{L_c}} \geq \gamma_L\right\}\right) \\ &\quad \times \left(1 - \Pr\left\{\gamma_{R_cL_c}^{AF,x_{H_c}} \geq \gamma_H, \gamma_{R_cL_c}^{AF,x_{L_c}} \geq \gamma_L\right\}\right) \\ &= \Theta_{L,1}^{AF}\Theta_{L,2}^{AF}, \end{aligned} \quad (75)$$

By using (9), (10), (22), and (23) and performing some algebraic manipulations similar to the derivation of $\mathcal{O}_H^{AF}$, $\Theta_{L,1}^{AF}$ and $\Theta_{L,2}^{AF}$ are respectively given by

$$\Theta_{L,1}^{AF} = \begin{cases} 1, & \gamma_H \geq \beta \\ F_Y(\omega_{HL}), & \gamma_H < \beta, \end{cases} \quad (76)$$

and

$$\Theta_{L,2}^{AF} = 1 - \widetilde{\sum}_{L,AF}^{(\chi_Z)} \Theta_{R,\omega_R}^{(\chi_Z)} \left(\frac{m_{RL}}{b\lambda_{RL}}\right)^{\frac{s+r+1}{2}}, \quad (77)$$

where

$$\widetilde{\sum}_{L,AF}^{(\chi_Z)} = \sum_{i=0}^{\chi_Z - 1} \sum_{U_R=i} \sum_{r=0}^{m_{RL}-1} \sum_{s=0}^{\varphi_R + m_{SR} - 1},$$

and

$$\begin{aligned} \Theta_{R,\omega_R}^{(\chi_Z)} &= \frac{2\Psi_R^{(\chi_Z)} \chi_Z m_{SR}^{m_{SR}}}{r!\Gamma(m_{SR})\lambda_{SR}^{m_{SR}}} \binom{\varphi_R + m_{SR} - 1}{s} \omega_R^{\frac{c_1}{2}} \\ &\quad \times \left[\frac{\lambda_{SR}}{(i+1)m_{SR}}\right]^{\frac{s-r+1}{2}} e^{-\frac{(i+1)m_{SR}\omega_R}{\lambda_{SR}}} \\ &\quad \times \mathcal{K}_{s-r+1}\left[2\sqrt{\frac{(i+1)\omega_R m_{SR} m_{RL}}{b\lambda_{SR}\lambda_{RL}}}\right]. \end{aligned}$$

Thus, $\mathcal{O}_L^{AF}$ is finally expressed as

$$\mathcal{O}_L^{AF} = \begin{cases} \Theta_{L,2}^{AF}, & \gamma_H \geq \beta \\ F_Y(\omega_{HL})\Theta_{L,2}^{AF}, & \gamma_H < \beta. \end{cases} \quad (78)$$

1) FOR SHS

In this case, the OP of SN L_c is given by

$$\mathcal{O}_L^{AF,SHS} = \begin{cases} \Theta_{L,2}^{AF,SHS}, & \gamma_H \geq \beta \\ F_Y^{SHS}(\omega_{HL})\Theta_{L,2}^{AF,SHS}, & \gamma_H < \beta, \end{cases} \quad (79)$$

where $F_Y^{SHS}(x)$ is obtained in (55) and $\Theta_{L,2}^{AF,SHS}$ has the following form:

$$\Theta_{L,2}^{AF,SHS} = 1 - \widetilde{\sum}_{L,AF}^{(K)} \Theta_{R,\omega_R}^{(K)} \left(\frac{m_{RL}}{b\lambda_{RL}}\right)^{\frac{s+r+1}{2}}. \quad (80)$$

2) FOR SRS

In the case of SRS, the OP of SN L_c is expressed as

$$\mathcal{O}_L^{AF,SRS} = \begin{cases} \Theta_{L,2}^{AF,SRS}, & \gamma_H \geq \beta \\ F_Y^{SRS}(\omega_{HL})\Theta_{L,2}^{AF,SRS}, & \gamma_H < \beta, \end{cases} \quad (81)$$

where $F_Y^{SRS}(x)$ is achieved as in (55) and $\Theta_{L,2}^{AF,SRS}$ is expressed as

$$\Theta_{L,2}^{AF,SRS} = 1 - \widetilde{\sum}_{L,AF}^{(NK)} \Theta_{R,\omega_R}^{(NK)} \left(\frac{m_{RL}}{b\lambda_{RL}}\right)^{\frac{s+r+1}{2}}. \quad (82)$$

3) FOR SLS

The OP of SN L_c in this case has the following form:

$$\mathcal{O}_L^{AF,SLS} = \begin{cases} \Theta_{L,2}^{AF,SLS}, & \gamma_H \geq \beta \\ F_Y^{SLS}(\omega_{HL})\Theta_{L,2}^{AF,SLS}, & \gamma_H < \beta, \end{cases} \quad (83)$$

where $\Theta_{L,2}^{AF,SLS} = \Theta_{L,2}^{AF,SHS}$ and $F_Y^{SLS}(x)$ are presented in (62).

VI. POWER-SPLITTING RATIO OPTIMIZATION AND EFFECTIVE COMMUNICATION STRATEGY

A. POWER-SPLITTING RATIO OPTIMIZATION

Based on the gradient method in [50], we present an algorithm to determine the optimal value of ρ, denoted by ρ_{opt}, with the aim of minimizing the OP. The algorithm is described in more detail as follows:

- We first determine the search direction for the algorithm. The natural selection for the search direction is the negative gradient [50]. Therefore, for a given starting point ρ_t, we have $\Delta\rho_t = -\nabla\mathcal{O}(\rho_t)$, where $\Delta\rho_t$ denotes the search direction and $\nabla\mathcal{O}(\rho_t)$ is the gradient of $\mathcal{O}(\rho_t)$, and $\mathcal{O}(\rho_t)$ is the considered OP. At ρ_{opt}, $\nabla\mathcal{O}(\rho_{opt}) = 0$.
- We next update the value of ρ_t as $\rho_{t+1} = \rho_t + k\Delta\rho_t$, where k is the step size. Note that $\rho_t < \rho_{t+1}$, whereas $\mathcal{O}(\rho_t) > \mathcal{O}(\rho_{t+1})$.
- The aforementioned iteration process will stop when Δ_{ρ_t} is smaller than a predetermined ending threshold e_t.

The algorithm is shown in **Algorithm 1**. Thus, to determine ρ_{opt}, we need to derive $\nabla\mathcal{O}(\rho)$.

Algorithm 1 Algorithm for Determining ρ_{opt}

Data : Predetermined system parameters, step size k, ending threshold e_t.

Result: ρ_{opt}

Set the initial step: $t \leftarrow 0$;
Select the starting point of ρ_t: $\rho_t \leftarrow 10^{-2}$;
Select the initial value of the search direction: $\Delta\rho_t \leftarrow 1$;
while $\Delta\rho_t > e_t$ **do**
    Update the search direction: $\Delta\rho_t \leftarrow -\nabla\mathcal{O}(\rho_t)$;
    Update ρ_t: $\rho_{t+1} \leftarrow \rho_t + k\Delta\rho_t$;
    Update t: $t \leftarrow t+1$;
end
Return ρ_t;

1) DERIVATION FOR $\nabla\mathcal{O}_H^{DF}(\rho)$

For $\mathcal{O}_H^{DF}$ in (39), $\Theta_{H,2}^{DF}$ can be rewritten with respect to ρ as follows:

$$\Theta_{H,2}^{DF}(\rho) = \widetilde{\sum}_{H,DF}^{(\chi_Z)} \Phi_H^{DF}\Phi(\rho), \tag{84}$$

where

$$\Phi(\rho) = \frac{1}{\rho^{j+r}}\Gamma\left[\phi, \frac{(i+1)m_{SR}\omega_{HL}}{\lambda_{SR}(1-\rho)}\right],$$

and

$$\Phi_H^{DF} = \frac{\chi_Z m_{SR}^{m_{SR}}}{\Gamma(m_{SR})\lambda_{SR}^{m_{SR}}}\frac{(-1)^r\Psi_R^{(\chi_Z)}}{j!r!}\left(\frac{m_{RH}\hat{g}_H}{\lambda_{RH}\eta\gamma_S}\right)^{j+r} \times\left[\frac{\lambda_{SR}}{(i+1)m_{SR}}\right]^{\phi}.$$

Therefore, the gradient of $\mathcal{O}_H^{DF}(\rho)$, i.e., $\nabla\mathcal{O}_H^{DF}(\rho)$, is given by

$$\nabla\mathcal{O}_H^{DF}(\rho) = \begin{cases} 0, & \gamma_H \geq \beta \\ 0, & \hat{\beta} \leq \gamma_H < \beta \\ -F_X\left(\frac{g_H}{\gamma_S}\right)\widetilde{\sum}_{H,DF}^{(\chi_Z)}\Phi_H^{DF}\dot{\Phi}(\rho), & \gamma_H < \min\left(\beta,\hat{\beta}\right), \end{cases} \tag{85}$$

where $\dot{\Phi}(\rho)$ is the first-order derivative of $\Phi(\rho)$, which is given by

$$\dot{\Phi}(\rho) = -\left\{\frac{j+r}{\rho^{j+r+1}}\Gamma\left[\phi, \frac{(i+1)m_{SR}\omega_{HL}}{\lambda_{SR}(1-\rho)}\right] + \left[\frac{(i+1)m_{SR}\omega_{HL}}{\lambda_{SR}}\right]^{\phi}\frac{e^{-\frac{(i+1)m_{SR}\omega_{HL}}{\lambda_{SR}(1-\rho)}}}{\rho^{j+r}(1-\rho)^{\phi+1}}\right\}. \tag{86}$$

By substituting the respective values of χ_X into $F_X\left(\frac{g_H}{\gamma_S}\right)$ and χ_Z into Φ_H^{DF} in (85), similar to subsection IV-A, we can easily obtain $\nabla\mathcal{O}_H^{DF}(\rho)$ in the cases of using SHS, SRS, and SLS.

2) DERIVATION FOR $\nabla\mathcal{O}_L^{DF}(\rho)$

For $\mathcal{O}_L^{DF}$ in (52), $\Theta_{L,12}^{DF}$ and $\Theta_{L,23}^{DF}$ can be rewritten with respect to ρ as follows:

$$\Theta_{L,12}^{DF}(\rho) = \widetilde{\sum}_{L,DF}^{(\chi_Z)}\left(\hat{g}_H\right)^{j+r}\Phi_L^{DF}\Phi(\rho), \tag{87}$$

and

$$\Theta_{L,23}^{DF}(\rho) = \widetilde{\sum}_{L,DF}^{(\chi_Z)}\left(\frac{\gamma_L}{b_{L_c}}\right)^{j+r}\Phi_L^{DF}\Phi(\rho), \tag{88}$$

where

$$\Phi_L^{DF} = \frac{\chi_Z m_{SR}^{m_{SR}}}{\Gamma(m_{SR})\lambda_{SR}^{m_{SR}}}\frac{(-1)^r\Psi_R^{(\chi_Z)}}{j!r!}\left(\frac{m_{RL}}{\eta\gamma_S\lambda_{RL}}\right)^{j+r} \times\left[\frac{\lambda_{SR}}{(i+1)m_{SR}}\right]^{\phi},$$

and $\Phi(\rho)$ is presented in (84).

Therefore, the gradient of $\mathcal{O}_L^{DF}(\rho)$, i.e., $\nabla\mathcal{O}_L^{DF}(\rho)$, is given by

$$\nabla\mathcal{O}_L^{DF}(\rho) = \begin{cases} 0, & \gamma_H \geq \beta \\ 0, & \hat{\beta} \leq \gamma_H < \beta \\ \dot{\Theta}_L^{DF}(\rho), & \gamma_H < \min\left(\beta,\hat{\beta}\right), \end{cases} \tag{89}$$

where

$$\dot{\Theta}_L^{DF}(\rho) = \begin{cases} -F_Y(\omega_{HL})\widetilde{\sum}_{L,DF}^{(\chi_Z)}\Phi_L^{DF} \times\left(\hat{g}_H\right)^{j+r}\dot{\Phi}(\rho), & \gamma_L < b_{L_c}\hat{g}_H \\ -F_Y(\omega_{HL})\widetilde{\sum}_{L,DF}^{(\chi_Z)}\Phi_L^{DF} \times\left(\frac{\gamma_L}{b_{L_c}}\right)^{j+r}\dot{\Phi}(\rho), & \gamma_L \geq b_{L_c}\hat{g}_H, \end{cases} \tag{90}$$

and $\dot{\Phi}(\rho)$ is shown in (86).

To obtain $\nabla\mathcal{O}_L^{DF}(\rho)$ when using SHS, SRS and SLS, we substitute the respective values of χ_Y and χ_Z into $\dot{\Theta}_L^{DF}(\rho)$ in (89) similar to subsection IV-B.

3) DERIVATION FOR $\nabla\mathcal{O}_H^{AF}(\rho)$

For $\mathcal{O}_H^{AF}$ in (69), $\Theta_{H,2}^{AF}$ can be rewritten with respect to ρ as

$$\Theta_{H,2}^{AF}(\rho) = 1 - \widetilde{\sum}_{H,AF}^{(\chi_Z)}\Phi_H^{AF}ABC_HD_H, \tag{91}$$

where

$$\Phi_H^{AF} = \left(\frac{1}{\Pi_H^{AF}}\right)^{s-r+1}\left(\frac{m_{RH}}{\eta\lambda_{RH}}\right)^{\frac{s+r+1}{2}}\binom{\varphi_R+m_{SR}-1}{s} \times\frac{2\Psi_R^{(\chi_Z)}\chi_Z m_{SR}^{m_{SR}}}{r!\Gamma(m_{SR})\lambda_{SR}^{m_{SR}}}\left[\frac{\lambda_{SR}}{(i+1)m_{SR}}\right]^{\frac{s-r+1}{2}}\left(\frac{g_H}{\gamma_S}\right)^{\frac{c_1}{2}},$$

$$D_H = \left[\frac{\Pi_H^{AF}}{\sqrt{\rho(1-\rho)}}\right]^{s-r+1}\mathcal{K}_{s-r+1}\left[\frac{\Pi_H^{AF}}{\sqrt{\rho(1-\rho)}}\right],$$

$A = \left(\frac{1}{\rho}\right)^r$, $B = \left(\frac{1}{1-\rho}\right)^{c_2}$, $C_H = e^{-\frac{d_H}{1-\rho}}$, $c_2 = \varphi_R + m_{SR} + r - s - 1$, $d_H = \frac{(i+1)m_{SR}g_H^{PSR}}{\gamma_S\lambda_{SR}}$, $\Pi_H^{AF} = 2\sqrt{\frac{(i+1)m_{SR}m_{RH}g_H}{\eta\gamma_S\lambda_{SR}\lambda_{RH}}}$, and c_1 is defined in (68).

Therefore, the gradient of $\mathcal{O}_H^{AF}(\rho)$, i.e., $\nabla\mathcal{O}_H^{AF}(\rho)$, is given by

$$\nabla\mathcal{O}_H^{AF}(\rho) = \begin{cases} \dot{\Theta}_{H,2}^{AF}, & \gamma_H \geq \beta \\ F_X\left(\frac{g_H}{\gamma_S}\right)\dot{\Theta}_{H,2}^{AF}, & \gamma_H < \beta, \end{cases} \tag{92}$$

where $\dot{\Theta}_{H,2}^{AF}(\rho)$ is expressed as

$$\begin{aligned}\dot{\Theta}_{H,2}^{AF}(\rho) &= \widetilde{\sum}_{H,AF}^{(\chi_Z)} \Phi_H^{AF} ABC_H \left\{ D_H \left[\frac{r}{\rho} - \frac{c_2}{1-\rho} + \frac{d_H}{(1-\rho)^2} \right] \right. \\ &\quad - \frac{(1-2\rho)\,\Pi_H^{AF}}{2[\rho(1-\rho)]^{3/2}} \left[\frac{\Pi_H^{AF}}{\sqrt{\rho(1-\rho)}} \right]^{s-r+1} \mathcal{K}_{s-r} \\ &\quad \left. \times \left[\frac{\Pi_H^{AF}}{\sqrt{\rho(1-\rho)}} \right] \right\}. \end{aligned} \tag{93}$$

By substituting the respective values of χ_X into $F_X\left(\frac{g_H}{\gamma_S}\right)$ and χ_Z into $\dot{\Theta}_{H,2}^{AF}(\rho)$ in (92), similar to subsection V-A, we can easily obtain $\nabla\mathcal{O}_H^{AF}(\rho)$ in the cases of using SHS, SRS, and SLS.

4) DERIVATION FOR $\mathcal{O}_L^{AF}(\rho)$

For $\mathcal{O}_L^{AF}$ in (78), $\Theta_{L,2}^{AF}$ can be rewritten with respect to ρ as

$$\Theta_{L,2}^{AF}(\rho) = 1 - \widetilde{\sum}_{L,AF}^{(\chi_Z)} \Phi_L^{AF} ABC_L D_L, \tag{94}$$

where

$$\begin{aligned}\Phi_L^{AF} &= \left(\frac{m_{RL}}{\eta\lambda_{RL}}\right)^{\frac{s+r+1}{2}} \left(\frac{1}{\Pi_L^{AF}}\right)^{s-r+1} \binom{\varphi_R + m_{SR} - 1}{s} \\ &\quad \times \frac{2\Psi_R^{(\chi_Z)}\chi_Z m_{SR}^{m_{SR}}}{r!\Gamma(m_{SR})\lambda_{SR}^{m_{SR}}} \left[\frac{\lambda_{SR}}{(i+1)m_{SR}}\right]^{\frac{s-r+1}{2}} (\omega_{HL})^{\frac{c_1}{2}}, \\ D_L &= \left[\frac{\Pi_L^{AF}}{\sqrt{\rho(1-\rho)}}\right]^{s-r+1} \mathcal{K}_{s-r+1}\left[\frac{\Pi_L^{AF}}{\sqrt{\rho(1-\rho)}}\right], \end{aligned}$$

$C_L = e^{-\frac{d_L}{1-\rho}}$, $d_L = \frac{(i+1)m_{SR}\omega_{HL}}{\lambda_{SR}}$, and $\Pi_L^{AF} = 2\sqrt{\frac{(i+1)m_{SR}m_{RL}\omega_{HL}}{\eta\lambda_{SR}\lambda_{RL}}}$.

Therefore, the gradient of $\mathcal{O}_L^{AF}(\rho)$, i.e., $\nabla\mathcal{O}_L^{AF}(\rho)$, is given by

$$\nabla\mathcal{O}_L^{AF}(\rho) = \begin{cases} \dot{\Theta}_{L,2}^{AF}, & \gamma_H \geq \beta \\ F_Y(\omega_{HL})\,\dot{\Theta}_{L,2}^{AF}, & \gamma_H < \beta, \end{cases} \tag{95}$$

where $\dot{\Theta}_{L,2}^{AF}(\rho)$ is expressed as

$$\begin{aligned}\dot{\Theta}_{L,2}^{AF,PSR}(\rho) &= \widetilde{\sum}_{L,AF}^{(\chi_Z)} \Phi_L^{AF} ABC_L \left\{ D_L \left[\frac{r}{\rho} - \frac{c_2}{1-\rho} + \frac{d_L}{(1-\rho)^2} \right] \right. \\ &\quad - \frac{(1-2\rho)\,\Pi_L^{AF}}{2[\rho(1-\rho)]^{3/2}} \left[\frac{\Pi_L^{AF}}{\sqrt{\rho(1-\rho)}} \right]^{s-r+1} \mathcal{K}_{s-r} \\ &\quad \left. \times \left[\frac{\Pi_L^{AF}}{\sqrt{\rho(1-\rho)}} \right] \right\}. \end{aligned} \tag{96}$$

By substituting the respective values of χ_Y into $F_Y(\omega_{HL})$ and χ_Z into $\dot{\Theta}_{L,2}^{AF}(\rho)$ in (95), similar to subsection V-B, we can easily obtain $\nabla\mathcal{O}_L^{AF}(\rho)$ in the cases of using SHS, SRS, and SLS.

B. EFFECTIVE COMMUNICATION STRATEGY

Algorithm 2 Algorithm for Determining γ_{S,I_c}

Data : Predetermined system parameters, step size k.
Result: γ_{S,I_c}

1 Set the initial step: $t \leftarrow 0$;
2 Select the starting point of average transmit SNR $\gamma_{S,t}$: $\gamma_{S,t} \leftarrow 0$ (dB);
3 Select the initial values of $\mathcal{O}_I^{\mathcal{A},\mathcal{B}}$ and $\mathcal{O}_I^{\mathcal{A},SRS}$: $\mathcal{O}_I^{\mathcal{A},\mathcal{B}} \leftarrow 1$ and $\mathcal{O}_I^{\mathcal{A},SRS} \leftarrow 0$;
4 **while** $\mathcal{O}_I^{\mathcal{A},\mathcal{B}} > \mathcal{O}_I^{\mathcal{A},SRS}$ **do**
5 Update $\mathcal{O}_I^{\mathcal{A},\mathcal{B}}$ and $\mathcal{O}_I^{\mathcal{A},SRS}$ with respect to $\gamma_{S,t}$;
6 Update $\gamma_{S,t}$: $\gamma_{S,t+1} \leftarrow \gamma_{S,t} + k$;
7 Update t: $t \leftarrow t + 1$;
8 **end**
9 Calculate γ_{S,I_c}: $\gamma_{S,I_c} \leftarrow \gamma_{S,t-1}$;
10 **Return** γ_{S,I_c};

Based on the obtained analytical results, we conclude that the best performance for SNs H_c and L_c is achieved by using SRS in the low-SNR regime. Meanwhile, the best performance is obtained by utilizing SHS for SN H_c and SLS for SN L_c in the high-SNR regime. This result will be clarified in the next section. Let γ_{S,I_c} ($I \in \{H, L\}$) denote the value of γ_S at which $\mathcal{O}_I^{\mathcal{A},\mathcal{B}} = \mathcal{O}_I^{\mathcal{A},SRS}$. Herein, $\mathcal{A} \in \{DF, AF\}$ and $\mathcal{B}$ stands for SHS when $I = H$ and SLS when $I = L$. Thus, to obtain the best performance, SRS should be used for SN I_c when $\gamma_S < \gamma_{S,I_c}$, whereas $\mathcal{B}$ should be used for SN I_c when $\gamma_S > \gamma_{S,I_c}$.

To determine γ_{S,I_c}, we propose the algorithm presented in **Algorithm 2**. Specifically, we first define a starting point of average transmit SNR, i.e., $\gamma_{S,t}$, at which $\mathcal{O}_I^{\mathcal{A},\mathcal{B}} > \mathcal{O}_I^{\mathcal{A},SRS}$. We then perform the iteration process as follows:

- We calculate $\mathcal{O}_I^{\mathcal{A},\mathcal{B}}$ and $\mathcal{O}_I^{\mathcal{A},SRS}$ with respect to $\gamma_{S,t}$.
- We next update the value of $\gamma_{S,t}$ as $\gamma_{S,t+1} = \gamma_{S,t} + k$, where k indicates the step size, and then we recalculate $\mathcal{O}_I^{\mathcal{A},\mathcal{B}}$ and $\mathcal{O}_I^{\mathcal{A},SRS}$ with respect to $\gamma_{S,t+1}$.
- The aforementioned iteration process will be stopped when $\mathcal{O}_I^{\mathcal{A},\mathcal{B}} < \mathcal{O}_I^{\mathcal{A},SRS}$.

VII. NUMERICAL RESULTS AND DISCUSSION

In this section, numerical results in terms of the OP at SNs H_c and L_c are provided to evaluate the performance of the

considered network. Without loss of generality, as widely used in previous works [23], [39], it is assumed that the coordinates of sink node S_c, relay R_c, SN H_c and SN L_c are $(0, 0)$, $(0.3, 0.3)$, $(0, 2)$, and $(2, 0)$, respectively. Therefore, we can obtain the normalized distances, i.e., d_{AB} $(A \neq B,\ A \in \{S, R\},\ B \in \{R, H, L\})$, by using the Euclidean metric. Furthermore, the predetermined simulation parameters are set as follows [11], [23], [39]: $N \in \{1, 2, 4\}$, $K \in \{1, 2, 4\}$, $P \in \{1, 2, 4\}$, $Q \in \{1, 2, 4\}$, the fading parameters $m_{AB} \in \{1, 2, 4\}$, the target data rate $R_H = R_L = 0.5$ (bps/Hz), the path loss exponents $\theta_{AB} = 2$, the energy conversion efficiency $\eta = 0.9$, the power-splitting ratio $\rho \in (0, 1)$, and the power allocation coefficients $a_{H_c} = b_{H_c} = 0.8$ and $a_{L_c} = b_{L_c} = 0.2$. For the infinite series in (39), (52), (85), and (89), we can truncate it to a specific number of terms to obtain the expected theoretical results. In this paper, we use the first 100 terms of the infinite sum, i.e., $r = 100$, for our analysis [39], [51].

A. COMPARISON OF THE ANTENNA-RELAY-DESTINATION SELECTION SOLUTIONS

This subsection intends to clarify how the three proposed antenna-relay-destination selection solutions (i.e., SHS, SRS, and SLS) affect the system performance. Specifically, Figs. 3 and 4 show the performance comparison of SHS, SRS, and SLS in the case of using the DF protocol at selected SNs H_c and L_c, respectively. Note that the performance of the random selection (RS) solution [23] is provided as a benchmark. As shown in these two figures, the SHS, SRS, and SLS solutions impart the SNs with better performance (i.e., lower OP) than does RS. This result can be explained as the channels from the sink node with the selected transmit antenna to the selected relay and SNs in SHS, SRS, and SLS are under a better condition compared with that in RS. This leads to the increase in system performance.

Considering the performance of SN H_c in Fig. 3, among the proposed solutions, SLS causes the worst performance since it only focuses on improving the channel quality of the $S_c \rightarrow L_c$ link. In the remaining two solutions, SRS outperforms SHS in the low-SNR regime and vice versa in the high-SNR regime. The reason for this result is that the signal quality on the $S_c \rightarrow H_c$ direct link in the low-SNR regime (i.e., low transmit power or high noise power) is reduced much faster than that in the high-SNR regime (i.e., high transmit power or low noise power) due to the path loss phenomenon. Therefore, the relaying transmission in the low-SNR area is more necessary compared with that in the high-SNR area.

With γ_{S,H_c} defined in VI-B, we can observe that among the two considered solutions (i.e., SHS and SRS), SRS should be used when $\gamma_S < \gamma_{S,H_c}$ and SHS should be used when $\gamma_S > \gamma_{S,H_c}$ to obtain the best performance for user H_c. To determine γ_{S,H_c}, as indicated in Fig. 3, **Algorithm 2** is utilized.

Considering the performance of SN L_c in Fig. 4, it is clear that the worst performance occurs when using SHS, whereas the best performance is obtained by using SRS in the low-SNR regime and by using SLS in the high-SNR regime.

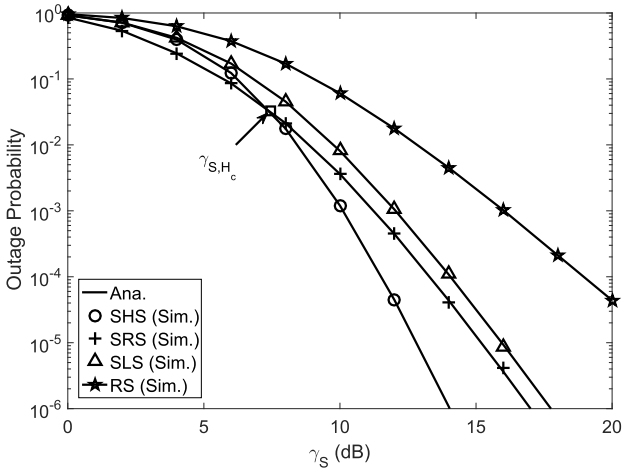

FIGURE 3. Comparison of the OP of SN H_c with the DF relaying protocol in the cases of using SHS, SRS, SLS, and RS schemes, in which $N = K = P = Q = 2$, $m_{AB} = 2$, and $\rho = 0.6$.

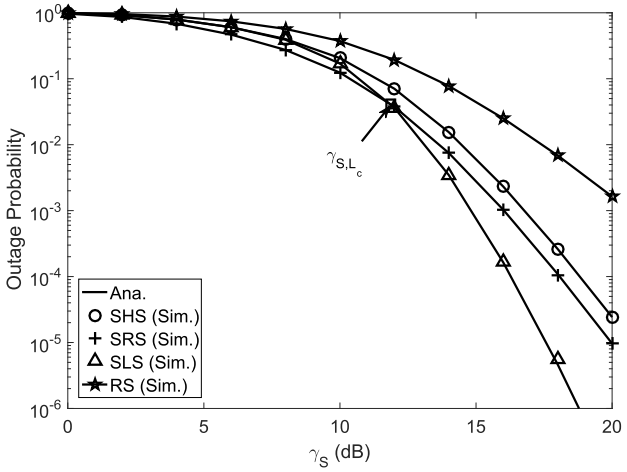

FIGURE 4. Comparison of the OP of SN L_c with the DF relaying protocol in the cases of using SHS, SRS, SLS, and RS schemes, in which $N = K = P = Q = 2$, $m_{AB} = 2$, and $\rho = 0.6$.

The reasons for these results are similar to the case of investigating the performance of SN H_c in Fig. 3. Furthermore, **Algorithm 2** can be used to determine γ_{S,L_c}, which is defined in VI-B. As shown in Fig. 4, to achieve the best performance for user L_c, SRS should be applied when $\gamma_S < \gamma_{S,L_c}$, and SLS should be used when $\gamma_S > \gamma_{S,L_c}$. Note that we do not consider the AF relaying protocol in this investigation since, according to our study, its effect on the system performance has the same trend as the DF scheme as shown in Fig. 5. This aims to avoid repetition.

B. EFFECT OF RELAYING STRATEGIES ON THE SYSTEM PERFORMANCE

This subsection considers how the two different relaying strategies (i.e., DF and AF) affect the system performance. Specifically, Fig. 5 shows the OP of SN H_c as a function of γ_S for the DF and AF relaying protocols in the cases of using SHS, SRS, and SLS. As shown in this figure, the OP of SN

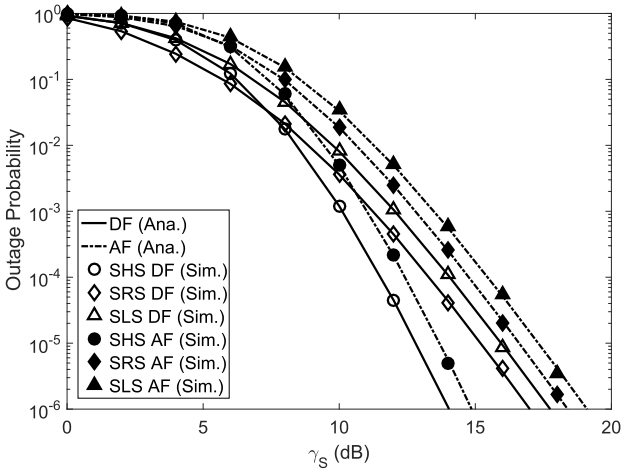

FIGURE 5. OP of SN H_c with the DF and AF relaying strategies in the cases of using SHS, SRS, and SLS, in which $N = K = P = Q = 2$, $m_{AB} = 2$, and $\rho = 0.6$.

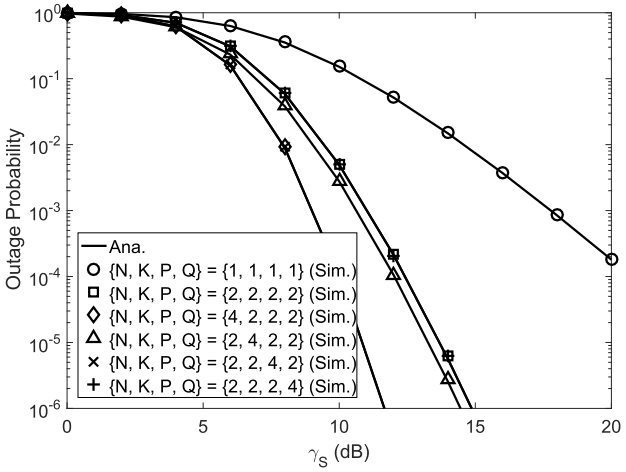

FIGURE 6. OP of SN H_c with AF and SHS solutions for different values of $\{N, K, P, Q\}$, in which $m_{AB} = 2$ and $\rho = 0.6$.

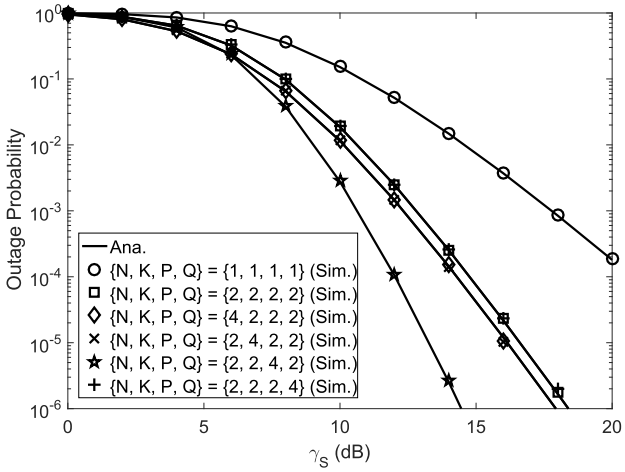

FIGURE 7. OP of SN H_c with AF and SRS solutions for different values of $\{N, K, P, Q\}$, in which $m_{AB} = 2$ and $\rho = 0.6$.

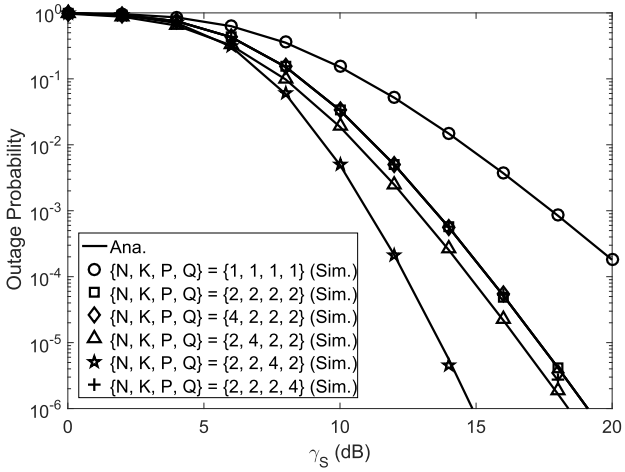

FIGURE 8. OP of SN H_c with AF and SLS solutions for different values of $\{N, K, P, Q\}$, in which $m_{AB} = 2$ and $\rho = 0.6$.

H_c with DF is lower than that with AF for all cases. In other words, the DF relaying strategy imparts SN H_c with better performance compared with the AF relaying protocol. This result can be explained as follows: with the DF protocol, relay R_c has to guarantee that it correctly receives the signals transmitted from sink node S_c (i.e., it successfully decodes the received signals) before performing relaying transmission. Meanwhile, with the AF protocol, relay R_c only amplifies the received signals and forwards the result to SN H_c. This does not help to achieve a further improvement in the reliability of SN H_c if relay R_c cannot successfully decode the received signals. Note that the performance of SN L_c is not investigated since it has the same behavior as that of H_c in this consideration.

C. EFFECTS OF THE NUMBERS OF TRANSMIT ANTENNAS, RELAYS, AND SENSOR NODES

This subsection investigates the effects of the numbers of transmit antennas (N), relays (K), SNs in cluster H (P), and SNs in cluster L (Q) on the system performance. Specifically, Figs. 6, 7, and 8 plot the OP of SN H_c as a function of γ_S with AF relaying protocol for different values of $\{N, K, P, Q\}$ in the cases of using SHS, SRS, and SLS, respectively. As shown in these figures, the variation of Q does not affect the performance of SN H_c. We can observe that the performance of SN H_c is the worst as $\{N, K, P\} = \{1, 1, 1\}$. Furthermore, in the low-SNR regime, its best performance is obtained by increasing K, N or K, and K corresponding to the cases of using SHS, SRS, and SLS. Meanwhile, in the high-SNR regime, this is achieved by increasing N or P, P, and P in the cases of applying SHS, SRS, and SLS, respectively. It can be explained similar to the comparison of the antenna-relay-destination selection strategies in subsection VII-A. Specifically, the relaying transmission in the low-SNR area is more necessary compared with that in the high-SNR area. Similar conclusions can be obtained when investigating the performance of SN L_c in this context, as shown in Figs. 9, 10, and 11, in which P does not affect the

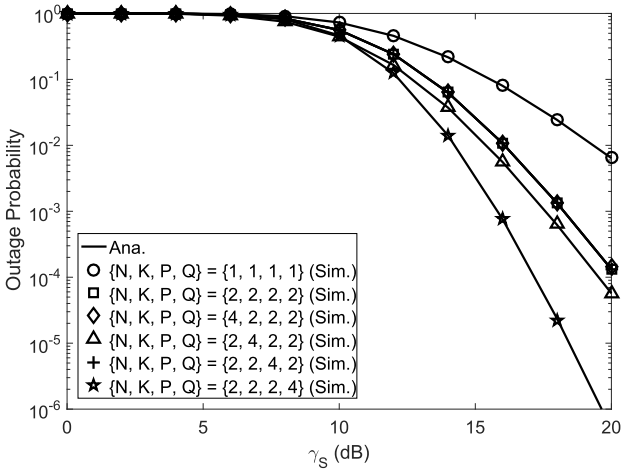

FIGURE 9. OP of SN L_c with AF and SHS solutions for different values of $\{N, K, P, Q\}$, in which $m_{AB} = 2$ and $\rho = 0.6$.

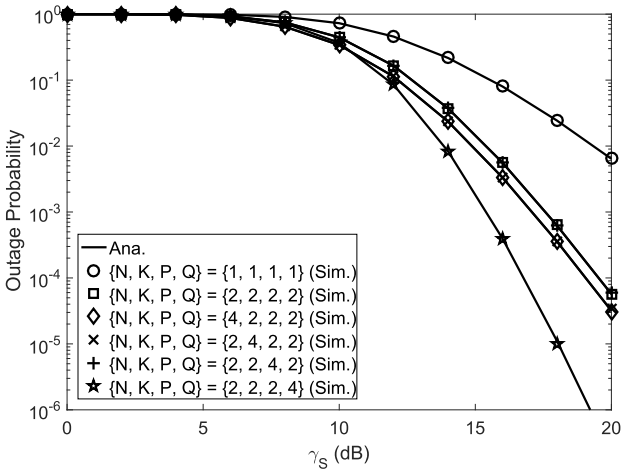

FIGURE 10. OP of SN L_c with AF and SRS solutions for different values of $\{N, K, P, Q\}$, in which $m_{AB} = 2$ and $\rho = 0.6$.

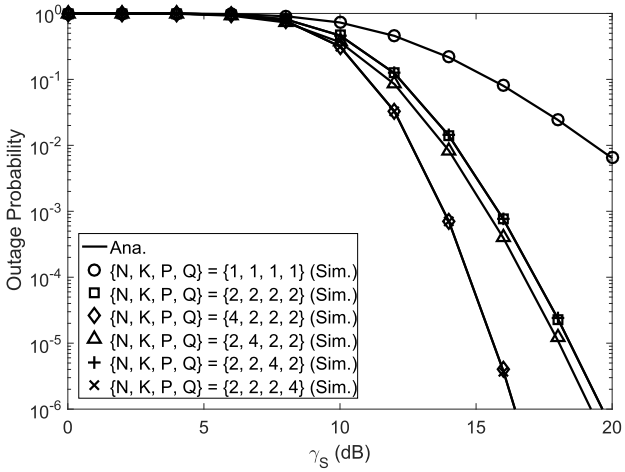

FIGURE 11. OP of SN L_c with AF and SLS solutions for different values of $\{N, K, P, Q\}$, in which $m_{AB} = 2$ and $\rho = 0.6$.

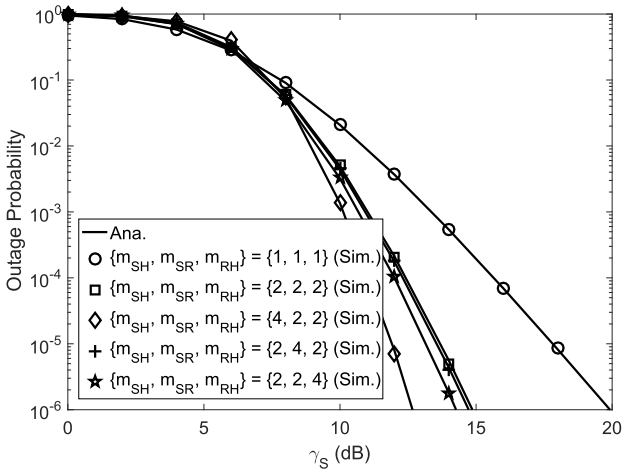

FIGURE 12. OP of SN H_c with AF and SHS solutions for different values of $\{m_{SH}; m_{SR}; m_{RH}\}$, in which $N = K = P = Q = 2$, $m_{SL} = m_{RL} = 2$, and $\rho = 0.6$.

performance of SN L_c. In particular, the best performance of SN L_c is achieved by increasing K for SHS, N or K for SRS, and K for SLS in the low-SNR regime and increasing Q for SHS, Q for SRS, and N or Q for SLS in the high-SNR regime.

D. EFFECT OF FADING PARAMETER

This subsection examines the effect of fading parameters (i.e., m_{SH}, m_{SR}, m_{SL}, m_{RH}, and m_{RL}) on the system performance. A Nakagami-m distribution is utilized to bring more general insights of the channel model. Specifically, in the case of $m = 1$, Nakagami-m fading corresponds to Rayleigh fading, whereas in the case of $m = (\kappa + 1)^2 / (2\kappa + 1)$, it approximates Rician fading with parameter κ. To avoid repetition, we only investigate the performance of SN H_c with AF and SHS solutions for different values of m_{SH}, m_{SR}, and m_{RH}, denoted by $\{m_{SH}, m_{SR}, m_{RH}\}$, as shown in Fig. 12. Notably, m_{SL} and m_{RL} do not affect the performance of SN H_c. When $\{m_{SH}, m_{SR}, m_{RH}\} = \{1, 1, 1\}$, i.e., the channels follow Rayleigh fading, the worst performance can be observed. Moreover, greater performance of SN H_c is obtained with the increases in m_{SH}, m_{SR}, and m_{RH} due to the better channel quality. Similar to the case of considering the effects of the numbers of transmit antennas, relays, and SNs on the system performance in VII-C, increasing the values of the parameters of the relaying link (i.e., m_{SR} and m_{RH}) helps to bring the best performance for SN H_c in the low-SNR regime. Meanwhile, increasing that of the direct link (i.e., m_{SH}) helps SN H_c reach the best performance in the high-SNR regime.

E. EFFECT OF POWER-SPLITTING RATIO ρ

This subsection illustrates how the power-splitting ratio affects the system performance. Specifically, Fig. 13 shows the OP of SN H_c as a function of ρ. To avoid repetition, the OP of SN L_c is not considered in this subsection because it has the same trend as that of SN H_c. As observed from this figure, the DF protocol outperforms the AF protocol for a fixed value of ρ. In each relaying protocol, the performance of SN H_c increases (i.e., OP decreases) in the order of SLS,

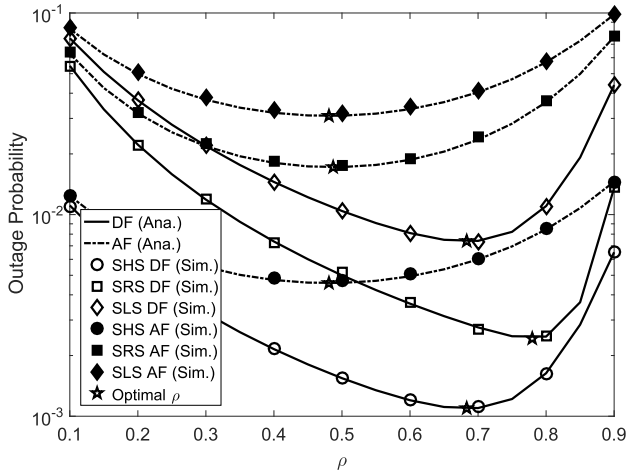

FIGURE 13. OP of SN H_c as a function of ρ, in which $N = K = P = Q = 2$, $m_{AB} = 2$, and $\gamma_S = 10$ (dB).

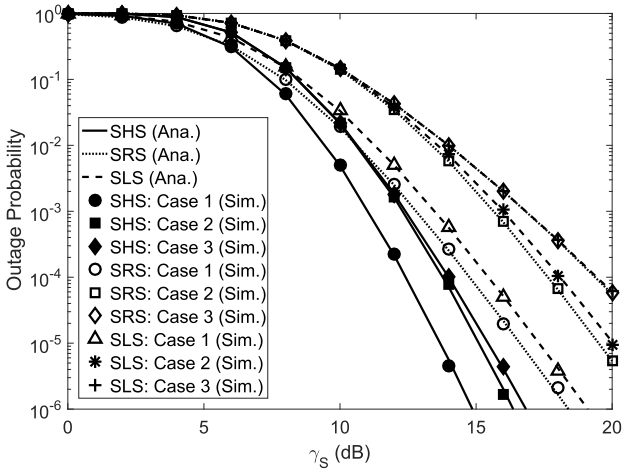

FIGURE 14. OP of SN H_c with AF protocol for different cases of d_{SR}, d_{RH}, and d_{RL}, in which $m_{AB} = 2$, $N = K = P = Q = 2$, and $\rho = 0.6$.

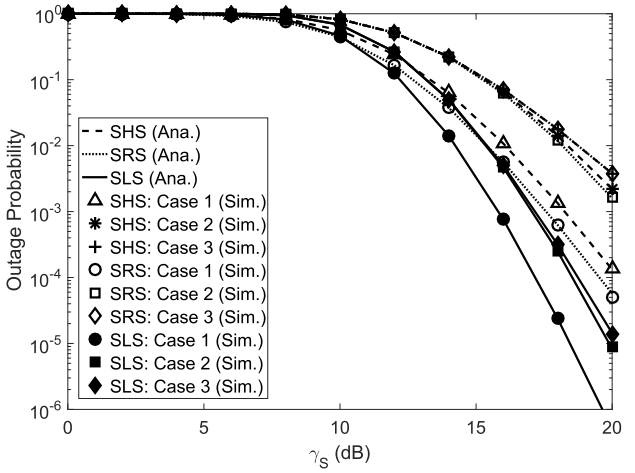

FIGURE 15. OP of SN L_c with AF protocol for different cases of d_{SR}, d_{RH}, and d_{RL}, in which $m_{AB} = 2$, $N = K = P = Q = 2$, and $\rho = 0.6$.

SRS, and SHS. Furthermore, the variation of ρ affects the OP in two opposite cases, as shown in Fig. 13. Specifically, in the first case, the increase in ρ results in the reduction of the OP due to the larger harvested energy at relay R_c. In the second case, the decrease in the power for $S_c \rightarrow R_c$ information transmission when ρ is much larger leads to the poor signal strength received at relay R_c. This causes an increase in the OP of SN H_c. Thus, it is clear that there is an optimal value of ρ where the OP obtains the minimum value. To determine the optimal value of ρ, the gradient-based algorithm is used, as shown in **Algorithm 1**.

F. EFFECT OF RELAY POSITION

This subsection depicts the effect of the relay position on the system performance. Specifically, we consider the following three cases: i) Case 1, where relay R_c is close to sink node S_c (i.e., d_{SR} is smaller than d_{RH} and d_{RL}); ii) Case 2, where relay R_c is right in the middle of sink node S_c and SNs H_c and L_c (i.e., $d_{SR} = d_{RH} = d_{RL}$); and iii) Case 3, where relay R_c is close to SNs H_c and L_c (i.e., d_{SR} is larger than d_{RH} and d_{RL}). In this context, we fix the coordinates of sink node S_c and SNs H_c and L_c as (0, 0), (0, 2), and (2, 0), respectively. Meanwhile, the coordinates of relay R_c vary with respect to Cases 1, 2, and 3 as (0.3, 0.3), (1, 1), and (2, 2), respectively. Furthermore, we set the first hop (i.e., the $S_c \rightarrow R_c$ link) and the second hop (i.e., the $R_c \rightarrow H_c$ and $R_c \rightarrow L_c$ links) in the same channel conditions (i.e., $m_{SR} = m_{RH} = m_{RL}$ and $\theta_{SR} = \theta_{RH} = \theta_{RL}$).

Considering this effect of SNs H_c and L_c on the system performance in Figs. 14 and 15, respectively, we see that for all solutions, SHS, SRS, and SLS, the best performance for both of the SNs, H_c and L_c, is achieved when relay R_c is close to sink node S_c (i.e., Case 1), whereas the worst performance occurs when relay R_c is close to the SNs (i.e., Case 3). This can be explained by how in the considered conditions, the first hop plays a more important role than does the second hop since it affects not only the amount of harvested energy but also the received signal quality at relay R_c. Therefore, we conclude that Case 1 outperforms Cases 2 and 3, similar to [21] and [52].

Moreover, for the approximation used in (66) with the AF protocol, we can observe from Figs. 5 to 15 that the analytical results are in a good agreement with the simulation results and that an excellent match between them can be obtained in the high SNR regime.

VIII. CONCLUSION

In this paper, we proposed a novel model of DL cooperative MISO WSN with NOMA and SWIPT over Nakagami-m fading. The system consists of a multiantenna sink node, an energy-limited relay cluster (R), a high-priority SN cluster (H), and a low-priority SN cluster (L). We investigated three antenna-relay-destination selection solutions, i.e., SHS, SRS, and SLS, by exploiting the direct link from the sink node to relays and SNs.

To characterize the system performance, we derived the closed-form expression of OP at the selected SNs for each proposed solution in the cases of using DF and

AF relaying strategies. Furthermore, we presented two algorithms, i.e., the power-splitting ratio optimization and the best antenna-relay-destination selection determination algorithms. The analytical results, which were verified by Monte Carlo simulations, showed that better system performance is obtained by increasing the fading parameter and the number of transmit antennas, relays, and SNs. Furthermore, for each selection solution, the DF protocol results in better performance for selected SNs than the AF protocol. Finally, in each investigated relaying strategy (i.e., DF or AF), SRS outperforms SHS and SLS in the low-SNR regime for both selected SNs. Meanwhile, in the high-SNR regime, the best solution for the selected SN in cluster H and that in cluster L are SHS and SLS, respectively.

For future work, we are investigating the worst SN selection based on the channel condition from the sink node to the SNs. Furthermore, we are considering a relay selection solution based on end-to-end SNR at the SNs to illustrate a practical implementation of the studied WSNs.

APPENDIX A
PROOF OF LEMMA 1

Using subsection III-A, the CDF of V, $F_V(x)$, is represented as [53]

$$F_V(x) = \left(1 - \sum_{i=0}^{m_{SA}-1} \frac{m_{SA}^i}{i!\lambda_{SA}^i} x^i e^{-\frac{m_{SA}x}{\lambda_{SA}}}\right)^{\chi_V}. \tag{97}$$

By applying binomial expansion [49, eq. (1.111)] to (97), $F_V(x)$ can be rewritten as

$$F_V(x) = \sum_{i=0}^{\chi_V} \binom{\chi_V}{i} (-1)^i e^{-\frac{im_{SA}x}{\lambda_{SA}}} \underbrace{\left(\sum_{j=0}^{m_{SA}-1} \frac{m_{SA}^j x^j}{j!\lambda_{SA}^j}\right)^i}_{\Theta}. \tag{98}$$

With the aid of the multinomial theorem, Θ in (98) is rewritten as

$$\Theta = \sum_{U_A=i} \Lambda_A x^{\varphi_A} \left[\prod_{j=0}^{m_{SA}-1} \left(\frac{m_{SA}^j}{j!\lambda_{SA}^j}\right)^{u_{A,j}}\right], \tag{99}$$

where $\Lambda_A = \binom{i}{u_{A,0}, \ldots, u_{A,m_{SA}-1}} = \frac{i!}{u_{A,0}! \ldots u_{A,m_{SA}-1}!}$.

By substituting (99) into (98), $F_V(x)$ is obtained as in (24). The proof is completed.

APPENDIX B
PROOF OF LEMMA 2

Using the definition of CDF, we first represent the CDF of W, $F_W(x)$, in the following form:

$$\begin{aligned} F_W(x) &= \Pr\left(\left|h_{R_c B_c}\right|^2 < x\right) \\ &= \sum_{k=1}^{K} \sum_{l=1}^{\chi_W} \Pr(R_c = k) \Pr(B_c = l) F_{\left|h_{R_k B_l}\right|^2}(x), \end{aligned} \tag{100}$$

where χ_W is expressed as

$$\chi_W = \begin{cases} P, & \text{if } W = Z_H \\ Q, & \text{if } W = Z_L. \end{cases} \tag{101}$$

Since all channels are considered to be i.i.d., we have $\Pr(R_c = k) = 1/K$ and $\Pr(B_c = l) = 1/\chi_W$ [54]. By substituting these results into (100), we obtain the final expression of $F_W(x)$ as in (30), and the proof is completed.

REFERENCES

[1] J. Wan *et al.*, "Software-defined industrial Internet of Things in the context of industry 4.0," *IEEE Sensors J.*, vol. 16, no. 20, pp. 7373–7380, Oct. 2016.

[2] X. Li, D. Li, J. Wan, A. Vasilakos, C. Lai, and S. Wang, "A review of industrial wireless networks in the context of industry 4.0," *Wireless Netw.*, vol. 23, no. 1, pp. 23–41, Jan. 2017.

[3] S. Wang, J. Wan, D. Li, and C. Zhang, "Implementing smart factory of industrie 4.0: An outlook," *Int. J. Distrib. Sensor Netw.*, vol. 12, no. 1, pp. 1–10, Apr. 2016.

[4] S. Wang, J. Wan, D. Zhang, D. Li, and C. Zhang, "Towards smart factory for industry 4.0: A self-organized multi-agent system with big data based feedback and coordination," *Comput. Netw.*, vol. 101, pp. 158–168, Jun. 2016.

[5] J. M. Williams *et al.*, "Weaving the wireless Web: Toward a low-power, dense wireless sensor network for the industrial IoT," *IEEE Microw. Mag*, vol. 18, no. 7, pp. 40–63, Nov./Dec. 2017.

[6] I. Khan, F. Belqasmi, R. Glitho, N. Crespi, M. Morrow, and P. Polakos, "Wireless sensor network virtualization: A survey," *IEEE Commun. Surveys Tuts.*, vol. 18, no. 1, pp. 553–576, 1st Quart., 2015.

[7] S. D. Trapasiya and H. B. Soni, "Energy efficient policy selection in wireless sensor network using cross layer approach," *IET Wireless Sensor Syst.*, vol. 7, no. 6, pp. 191–197, Dec. 2017.

[8] H.-H. Liu, J.-J. Su, and C.-F. Chou, "On energy-efficient straight-line routing protocol for wireless sensor networks," *IEEE Syst. J.*, vol. 11, no. 4, pp. 2374–2382, Dec. 2017.

[9] Y. Li, N. Yu, W. Zhang, W. Zhao, X. You, and M. Daneshmand, "Enhancing the performance of LEACH protocol in wireless sensor networks," in *Proc. IEEE Conf. Comput. Commun. Workshops*, Shanghai, China, Apr. 2011, pp. 223–228.

[10] M. Chincoli and A. Liotta, "Self-learning power control in wireless sensor networks," *Sensors*, vol. 18, no. 2, p. 375, Jan. 2018.

[11] H. Tran, J. Åkerberg, M. Björkman, and H.-V. Tran, "RF energy harvesting: An analysis of wireless sensor networks for reliable communication," *J. Wireless Netw.*, pp. 1–15, Jun. 2017, doi: 10.1007/s11276-017-1546-6.

[12] D.-B. Ha, D.-D. Tran, H.-V. Tran, and E.-K. Hong, "Performance of amplify-and-forward relaying with wireless power transfer over dissimilar channels," *Elektronika IR Elektrotechnika*, vol. 21, no. 5, pp. 90–95, Oct. 2015.

[13] D.-D. Tran, H.-V. Tran, D.-B. Ha, H. Tran, and G. Kaddoum, "Performance analysis of two-way relaying system with RF-EH and multiple antennas," in *Proc. IEEE 84th Veh. Technol. Conf. (VTC)*, Montreal, QC, Canada, Sep. 2016, pp. 1–5.

[14] V. N. Vo, T. G. Nguyen, C. So-In, and D.-B. Ha, "Secrecy performance analysis of energy harvesting wireless sensor networks with a friendly jammer," *IEEE Access*, vol. 5, pp. 25196–25206, 2017.

[15] D. Niyato, D. I. Kim, M. Maso, and Z. Han, "Wireless powered communication networks: Research directions and technological approaches," *IEEE Wireless Commun.*, vol. 24, no. 6, pp. 88–97, Dec. 2017.

[16] V. N. Vo, T. G. Nguyen, C. So-In, Z. A. Baig, and S. Sanguanpong, "Secrecy outage performance analysis for energy harvesting sensor networks with a jammer using relay selection strategy," *IEEE Access*, vol. 6, pp. 23406–23419, 2018, doi: 10.1109/ACCESS.2018.2829485.

[17] I. Krikidis, S. Timotheou, S. Nikolaou, G. Zheng, D. W. K. Ng, and R. Schober, "Simultaneous wireless information and power transfer in modern communication systems," *IEEE Commun. Mag.*, vol. 52, no. 11, pp. 104–110, Nov. 2014.

[18] T. D. P. Perera, D. N. K. Jayakody, S. K. Sharma, S. Chatzinotas, and J. Li, "Simultaneous wireless information and power transfer (SWIPT): Recent advances and future challenges," *IEEE Commun. Surveys Tuts.*, vol. 20, no. 1, pp. 264–302, 4th Quart., 2017.

[19] S. H. Mousavi, J. Haghighat, W. Hamouda, and R. Dastbasteh, "Analysis of a subset selection scheme for wireless sensor networks in time-varying fading channels," *IEEE Trans. Signal Process.*, vol. 64, no. 9, pp. 2193–2208, May 2016.
[20] J. Haghighat, M. Eslami, and W. Hamouda, "Relay pre-selection for reducing CSI transmission in wireless sensor networks," *IEEE Commun. Lett.*, vol. 20, no. 9, pp. 1828–1831, Sep. 2016.
[21] A. A. Nasir, X. Zhou, S. Durrani, and R. A. Kennedy, "Relaying protocols for wireless energy harvesting and information processing," *IEEE Trans. Wireless Commun.*, vol. 12, no. 7, pp. 3622–3636, Jul. 2013.
[22] K. Xiong, P. Fan, C. Zhang, and K. B. Letaief, "Wireless information and energy transfer for two-hop non-regenerative MIMO-OFDM relay networks," *IEEE J. Sel. Areas Commun.*, vol. 33, no. 8, pp. 1595–1611, Aug. 2015.
[23] N. T. Do, D. B. da Costa, T. Q. Duong, and B. An, "A BNBF user selection scheme for NOMA-based cooperative relaying systems with SWIPT," *IEEE Commun. Lett.*, vol. 21, no. 3, pp. 664–667, Mar. 2017.
[24] Y.-K. Hua, A.-C. Pang, P.-C. Hsiu, W. Zhuang, and P. Liu, "Distributed throughput optimization for ZigBee cluster-tree networks," *IEEE Trans. Parallel Distrib. Syst.*, vol. 23, no. 3, pp. 513–520, Mar. 2012.
[25] S. Rachamalla and A. Kancharla, "Survey of real-time routing protocols for wireless sensor networks," *Int. J. Comput. Sci. Eng. Surv.*, vol. 4, no. 3, pp. 35–44, Jun. 2013.
[26] A. Alanazi and K. Elleithy, "Real-time QoS routing protocols in wireless multimedia sensor networks: Study and analysis," *Sensors*, vol. 15, no. 9, pp. 22209–22233, Sep. 2015.
[27] J. Zhu, Y. Song, D. Jiang, and H. Song, "A new deep-q-learning-based transmission scheduling mechanism for the cognitive Internet of Things," *IEEE Internet Things J.*, vol. 5, no. 4, pp. 2375–2385, Aug. 2018, doi: 10.1109/JIOT.2017.2759728.
[28] D. Zhai, R. Zhang, L. Cai, B. Li, and Y. Jiang, "Energy-efficient user scheduling and power allocation for noma-based wireless networks with massive IoT devices," *IEEE Internet Things J.*, vol. 5, no. 3, pp. 1857–1868, Jun. 2018.
[29] Z. Ding, Z. Yang, P. Fan, and H. V. Poor, "On the performance of non-orthogonal multiple access in 5G systems with randomly deployed users," *IEEE Signal Process. Lett.*, vol. 21, no. 12, pp. 1501–1505, Dec. 2014.
[30] Y. Liu, Z. Ding, M. Elkashlan, and H. V. Poor, "Cooperative non-orthogonal multiple access with simultaneous wireless information and power transfer," *IEEE J. Sel. Areas Commun.*, vol. 34, no. 4, pp. 938–953, Apr. 2016.
[31] D.-D. Tran and D.-B. Ha, "Secrecy performance analysis of QoS-based non-orthogonal multiple access networks over Nakagami-m fading," in *Proc. 2nd Int. Conf. Recent Adv. Signal Process., Telecommun. Comput. (SigTelCom)*, Ho Chi Minh City, Vietnam, Jan. 2018, pp. 187–191.
[32] Z. Chen, Z. Ding, X. Dai, and R. Zhang, "A mathematical proof of the superiority of NOMA compared to conventional OMA," *IEEE Trans. Signal Process.*, to be published. [Online]. Available: https://arxiv.org/abs/1612.01069
[33] M. Zeng, A. Yadav, O. A. Dobre, G. I. Tsiropoulos, and H. V. Poor, "On the sum rate of MIMO-NOMA and MIMO-OMA systems," *IEEE Wireless Commun. Lett.*, vol. 6, no. 4, pp. 534–537, Aug. 2017.
[34] Y. Saito, Y. Kishiyama, A. Benjebbour, T. Nakamura, A. Li, and K. Higuchi, "Non-orthogonal multiple access (NOMA) for cellular future radio access," in *Proc. IEEE 77th Veh. Technol. Conf.*, Dresden, Germany, Jun. 2013, pp. 1–5.
[35] T. Shimojo, A. Umesh, D. Fujishima, and A. Minokuchi, "Special articles on 5G technologies toward 2020 deployment," *NTT DOCOMO Tech. J.*, vol. 17, no. 4, pp. 50–59, 2016.
[36] L. Dai, B. Wang, Y. Yuan, S. Han, C.-L. I, and Z. Wang, "Non-orthogonal multiple access for 5G: Solutions, challenges, opportunities, and future research trends," *IEEE Commun. Mag.*, vol. 53, no. 9, pp. 74–81, Sep. 2015.
[37] A. Anwar, B.-C. Seet, and Z. Ding, "Non-orthogonal multiple access for ubiquitous wireless sensor networks," *Sensors*, vol. 18, no. 2, p. 516, Feb. 2018.
[38] M. Song and M. Zheng, "Energy efficiency optimization for wireless powered sensor networks with nonorthogonal multiple access," *IEEE Sensors Lett.*, vol. 2, no. 1, Mar. 2018, Art. no. 7500304.
[39] D.-B. Ha and S. Q. Nguyen, "Outage performance of energy harvesting DF relaying NOMA networks," *Mobile Netw. Appl.*, pp. 1–14, Oct. 2017.
[40] T. N. Do, D. B. da Costa, T. Q. Duong, and B. An, "Improving the performance of cell-edge users in MISO-NOMA systems using TAS and SWIPT-based cooperative transmissions," *IEEE Trans. Green Commun. Netw.*, vol. 2, no. 1, pp. 49–62, Mar. 2018.
[41] O. K. Rayel, G. Brante, J. L. Rebelatto, R. D. Souza, and M. A. Imran, "Energy efficiency-spectral efficiency trade-off of transmit antenna selection," *IEEE Trans. Commun.*, vol. 62, no. 12, pp. 4293–4303, Dec. 2014.
[42] D. C. González, D. B. da Costa, and J. C. S. S. Filho, "Distributed TAS/MRC and TAS/SC schemes for fixed-gain AF systems with multiantenna relay: Outage performance," *IEEE Trans. Wireless Commun.*, vol. 15, no. 6, pp. 4380–4392, Jun. 2016.
[43] G. Pan *et al.*, "On secrecy performance of MISO SWIPT systems with TAS and imperfect CSI," *IEEE Trans. Commun.*, vol. 64, no. 9, pp. 3831–3843, Sep. 2016.
[44] S. Kisseleff, X. Chen, I. F. Akyildiz, and W. H. Gerstacker, "Efficient charging of access limited wireless underground sensor networks," *IEEE Trans. Commun.*, vol. 64, no. 5, pp. 2130–2142, May 2016.
[45] G. Pan, H. Lei, Y. Yuan, and Z. Ding, "Performance analysis and optimization for SWIPT wireless sensor networks," *IEEE Trans. Commun.*, vol. 65, no. 5, pp. 2291–2302, May 2017.
[46] S. Guo, F. Wang, Y. Yang, and B. Xiao, "Energy-efficient cooperative transmission for simultaneous wireless information and power transfer in clustered wireless sensor networks," *IEEE Trans. Commun.*, vol. 63, no. 11, pp. 4405–4417, Nov. 2015.
[47] T. Liu, X. Wang, and L. Zheng, "A cooperative SWIPT scheme for wirelessly powered sensor networks," *IEEE Trans. Commun.*, vol. 65, no. 6, pp. 2740–2752, Jun. 2017.
[48] R. Zouheir and M. S. Alouini, "On the capacity of Nakagami-m fading channels with full channel state information at low SNR," *IEEE Wireless Commun. Lett.*, vol. 1, no. 3, pp. 253–256, Apr. 2012.
[49] I. Gradshteyn and I. Ryzhik, *Table of Integrals, Series, and Products*, 7th ed. New York, NY, USA: Academic, Mar. 2007.
[50] S. Boyd and L. Vandenberghe, *Convex Optimization*. Cambridge, U.K.: Cambridge Univ. Press, 2004.
[51] H. A. Suraweera, G. K. Karagiannidis, and P. J. Smith, "Performance analysis of the dual-hop asymmetric fading channel," *IEEE Trans. Wireless Commun.*, vol. 8, no. 6, pp. 2783–2788, Jun. 2009.
[52] G. Zhu, C. Zhong, H. A. Suraweera, G. K. Karagiannidis, Z. Zhang, and T. A. Tsiftsis, "Wireless information and power transfer in relay systems with multiple antennas and interference," *IEEE Trans. Commun.*, vol. 63, no. 4, pp. 1400–1418, Apr. 2015.
[53] X. Zhang, X. Zhou, and M. R. McKay, "Enhancing secrecy with multi-antenna transmission in wireless ad hoc networks," *IEEE Trans. Inf. Forensics Security*, vol. 8, no. 11, pp. 1802–1814, Nov. 2013.
[54] Y. Zou, X. Wang, and W. Shen, "Optimal relay selection for physical layer security in cooperative wireless networks," *IEEE J. Sel. Areas Commun.*, vol. 31, no. 10, pp. 2099–2111, Oct. 2013.

DUC-DUNG TRAN received the B.E. degree in electronics and telecommunications from the Hue University of Sciences, Vietnam, in 2013, and the M.Sc. degree in computer sciences from Duy Tan University, Danang, Vietnam, in 2016. From 2013 to 2014, he was an Assistant Researcher with the Institute of R&D, Duy Tan University. He joined the Faculty of Electrical and Electronics Engineering, Duy Tan University, in 2015. His research interests include secrecy physical layer communications, wireless communications, multiple-input multiple-output systems, and wireless energy harvesting networks.

DAC-BINH HA received the B.S. degree in radio techniques and the M.S. and Ph.D. degrees in communications and information systems from the Huazhong University of Science and Technology, China, in 1997, 2006, and 2009, respectively. He is currently the Dean of the Faculty of Electrical and Electronics Engineering, Duy Tan University, Vietnam.

VAN NHAN VO received the B.S. and M.S. degrees in computer science from Danang University, Duy Tan University, Danang, Vietnam, in 2006 and 2014, respectively. He is currently pursuing the Ph.D. degree with the Department of Computer Science, Faculty of Science, Khon Kaen University, Thailand. Since 2009, he has taught and studied at Duy Tan University. His research interests include information security, physical layer secrecy, radio-frequency energy harvesting, wireless sensor networks, and the security of other advanced communication systems. He is a member of Cisco Systems, Juniper Systems, and ComPTIA Systems.

CHAKCHAI SO-IN (SM'14) received the Ph.D. degree in computer engineering from Washington University, St. Louis, MO, USA, in 2010. He was an Intern with CNAP-NTU (SG), Cisco Systems, WiMAX Forums, and Bell Labs, USA. He is currently a Professor with the Department of Computer Science, Khon Kaen University. He has authored over 85 publications and 10 books, including some in IEEE JSAC, IEEE magazines, and Computer Network/Network Security Labs. His research interests include mobile computing, wireless/sensor networks, signal processing, and computer networking and security. He is a Senior Member of ACM. He has served as an Editor at SpringerPlus, PeerJ, and ECTI-CIT and as a Committee Member for many conferences/journals, such as Globecom, ICC, VTC, WCNC, ICNP, ICNC, PIMRC, IEEE TRANSACTIONS, IEEE letter/magazines, *Computer Networks*, and *Computer Communications*.

HUNG TRAN received the B.S. and M.S. degrees in information technology from Vietnam National University, Hanoi, in 2002 and 2006, respectively, and the Ph.D. degree from the School of Computing, Blekinge Institute of Technology, Karlskrona, Sweden, in 2013. In 2014, he joined the Electrical Engineering Department, École de Technologie Supérieure, Montreal, QC, Canada. He is currently a Post-Doctoral Researcher with Mälardalen University, Sweden. His research interests include cognitive radio networks, cooperative communication systems, millimeter-wave communications, energy harvesting, and security communications at the physical layer.

TRI GIA NGUYEN received the B.Ed. degree from the Hue University of Education in 2011, the M.Sc. degree from Duy Tan University, Vietnam, in 2013, and the Ph.D. degree from Khon Kaen University, Thailand, in 2017, all in computer science. He is currently a Post-Doctoral Researcher with the Department of Computer Science, Faculty of Science, Khon Kaen University. His research interests include Internet of Things, sensor networks, wireless communications, wireless energy harvesting networks, mobile computing, computer systems, network security, and modeling and analysis.

ZUBAIR AHMED BAIG is currently a Senior Research Scientist of cyber security with CSIRO, Australia. He has authored over 50 journal and conference articles and book chapters. His research interests are in the areas of cyber security, artificial intelligence, smart cities, and the Internet of Things. He is currently serving as an Editor of the *IET Wireless Sensor Systems* journal and a review journal PSU (Emerald Publishing House). He has served on numerous technical program committees of international conferences and has delivered numerous keynote talks on cyber security.

SURASAK SANGUANPONG received the B.Eng. and M.Eng. degrees in electrical engineering from Kasetsart University in 1985 and 1987, respectively. He is currently an Associate Professor with the Department of Computer Engineering and the Director of the Applied Network Research Laboratory, Kasetsart University. His research focuses on network measurement, Internet security, and high-speed networking.